ANNUAL REVIEWS

Annual Review of Vision Science

Feature Detection by Retinal Ganglion Cells

Daniel Kerschensteiner

John F. Hardesty, MD, Department of Ophthalmology and Visual Sciences; Department of Neuroscience; Department of Biomedical Engineering; and Hope Center for Neurological Disorders, Washington University School of Medicine, Saint Louis, Missouri, USA; email: kerschensteinerd@wustl.edu

Annu. Rev. Vis. Sci. 2022. 8:3.1–3.35

The *Annual Review of Vision Science* is online at vision.annualreviews.org

https://doi.org/10.1146/annurev-vision-100419-112009

Keywords

receptive field, direction selectivity, object motion, looming, orientation selectivity, luminance contrast

Abstract

Retinal circuits transform the pixel representation of photoreceptors into the feature representations of ganglion cells, whose axons transmit these representations to the brain. Functional, morphological, and transcriptomic surveys have identified more than 40 retinal ganglion cell (RGC) types in mice. RGCs extract features of varying complexity; some simply signal local differences in brightness (i.e., luminance contrast), whereas others detect specific motion trajectories. To understand the retina, we need to know how retinal circuits give rise to the diverse RGC feature representations. A catalog of the RGC feature set, in turn, is fundamental to understanding visual processing in the brain. Anterograde tracing indicates that RGCs innervate more than 50 areas in the mouse brain. Current maps connecting RGC types to brain areas are rudimentary, as is our understanding of how retinal signals are transformed downstream to guide behavior. In this article, I review the feature selectivities of mouse RGCs, how they arise, and how they are utilized downstream. Not only is knowledge of the behavioral purpose of RGC signals critical for understanding the retinal contributions to vision; it can also guide us to the most relevant areas of visual feature space.

1. INTRODUCTION

Light traverses the circuitry of the retina before the outer segments of photoreceptors absorb it. The rods and two types of mouse cones differ in absolute and spectral sensitivities but uniformly reduce glutamate release in response to light (Masland 2001, Wässle 2004). This synaptic signal is picked up by second-order bipolar cells, which transmit information from the outer plexiform layer (OPL) to the inner plexiform layer (IPL) (Euler et al. 2014) (**Figure 1*a***). In the IPL, bipolar cell axons innervate amacrine cells and RGCs, the retina's output neurons (Demb & Singer 2015, Diamond 2017).

One of the retina's most striking features is its neuronal diversity (**Figure 1*b***). The mouse retina contains three types of photoreceptors (one rod, two cones); one horizontal cell type, which provides feedback to photoreceptors; 15 bipolar cell types; 63 amacrine cell types; and more than 40 RGC types (Baden et al. 2016, Bae et al. 2018, Helmstaedter et al. 2013, Rheaume et al. 2018,

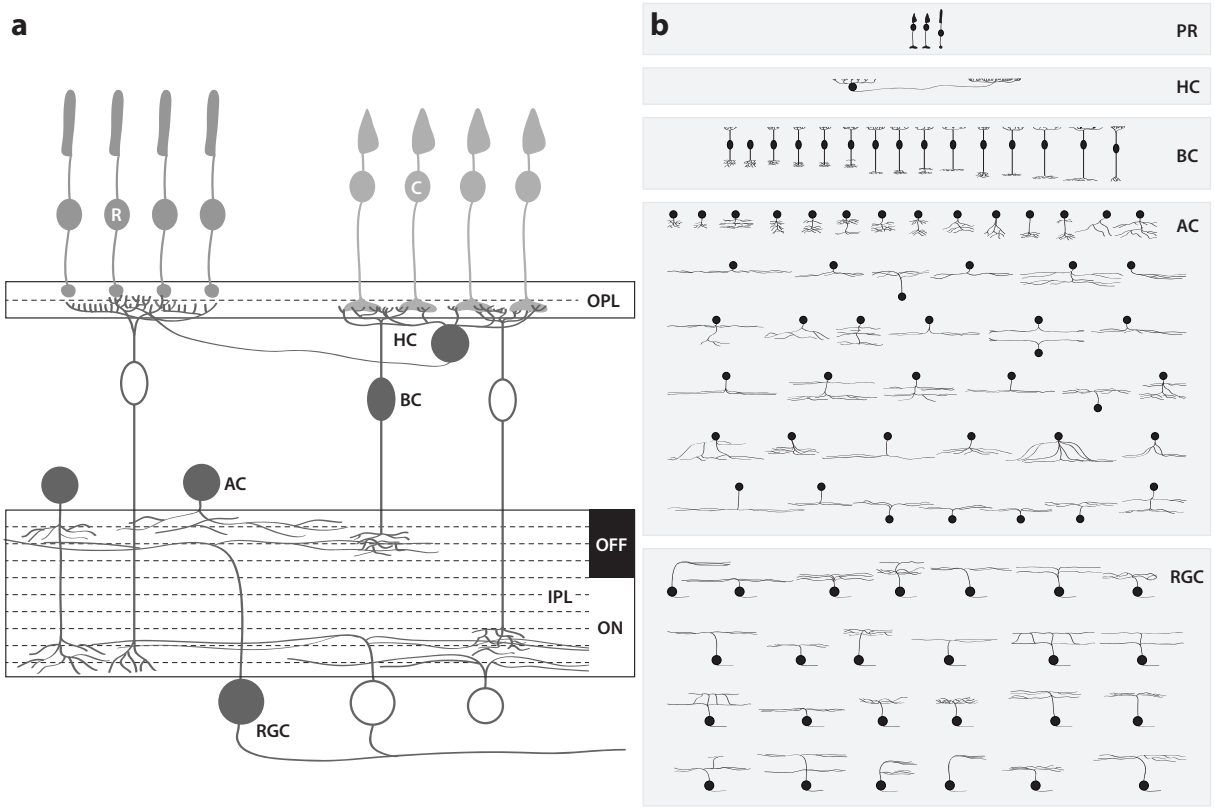

Figure 1

Retinal circuit architecture and neuron complement. (*a*) Simplified schematic of the retina. Rod (R) and cone (C) photoreceptors (PRs) in the outer retina translate changes in photon flux into changes in glutamate release onto bipolar cell (BC) dendrites and horizontal cell (HC) axons (rods) and dendrites (cones) in the outer plexiform layer (OPL). ON bipolar cells (open somas) invert the sign of the PR response, depolarize to light, and stratify their axons in the inner three-fifths of the inner plexiform layer (IPL). OFF bipolar cells (filled somas) depolarize to light decrements and stratify their axons in the outer two-fifths of the IPL. Bipolar cells synapse onto amacrine cells (ACs), which make up a diverse class of retinal interneurons, and retinal ganglion cells (RGCs), the eye's output neurons. (*b*) A catalog of the diverse cell types within the five main neuron classes. The mouse retina contains three types of PRs (two cones, one rod), one HC type, 15 BC types, 63 AC types, and more than 40 RGC types (subsets of the latter two are shown in the figure).

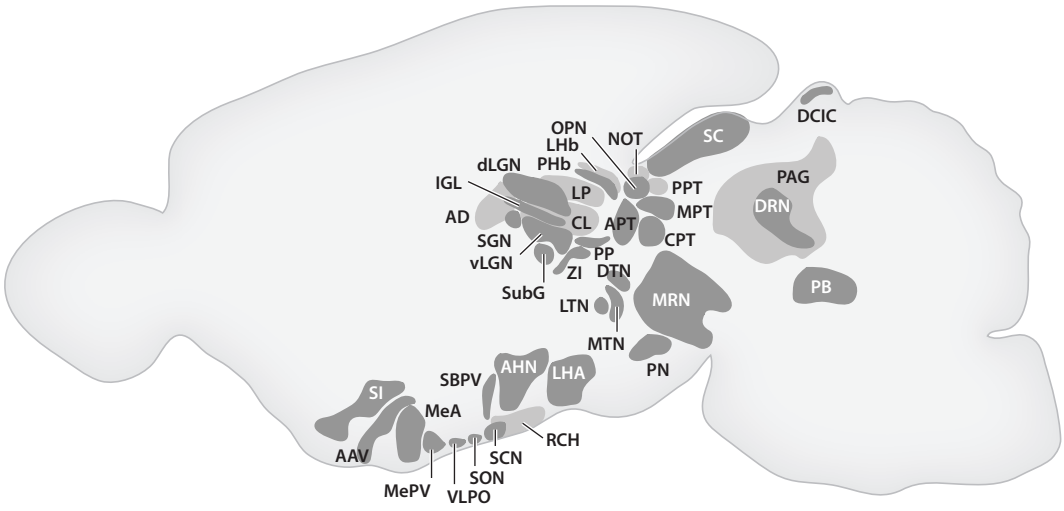

Figure 2

Retinorecipient brain areas. As illustrated, diverse brain areas receive RGC input. Abbreviations: AAV, anterior amygdaloid area, ventral; AD, anterodorsal thalamic nucleus; AHN, anterior hypothalamic area; APT, anterior pretectal nucleus; CL, centrolateral thalamic nucleus; CPT, commissural pretectal nucleus; DCIC, dorsal cortex of the inferior colliculus; dLGN, dorsolateral geniculate nucleus of the thalamus; DRN, dorsal raphe nucleus; DTN, dorsal terminal nucleus; IGL, intergeniculate leaflet; LHA, lateral hypothalamic area; LHb, lateral habenula; LHN, lateral hypothalamic area; LP, lateral posterior nucleus of the thalamus; LTN, lateral terminal nucleus; MeA, medial amygdala, anterior; MePV, medial amygdala, posteroventral; MPT, medial pretectal nucleus; MRN, midbrain reticular nucleus; MTN, medial terminal nucleus; NOT, nucleus of the optic tract; OPN, olivary pretectal nucleus; PAG, periaqueductal gray; PB, parabrachial nucleus; PHb, perihabenular nucleus; PN, paranigral nucleus; PP, peripeduncular nucleus; PPT, posterior pretectal nucleus; RCH, retrochiasmatic area; RGC, retinal ganglion cell; SGN, suprageniculate nucleus; SBPV, subparaventricular zone; SC, superior colliculus; SCN, suprachiasmatic nucleus; SI, substantia innominate; SON, supraoptic nucleus; SubG, subgeniculate nucleus; vLGN, ventrolateral geniculate nucleus; VLPO, ventrolateral preoptic area; ZI, zona incerta.

Shekhar et al. 2016, Tran et al. 2019, Yan et al. 2020). The assembly of diverse neurons into specific circuits is aided by the laminar architecture of the retina (Sanes & Zipursky 2010). The OPL and the IPL are divided into sublayers. Rods form synapses with their partners (horizontal cell axons and rod bipolar cells) in the outer OPL, whereas cones contact their partners (horizontal cell dendrites and cone bipolar cells) in the inner OPL. The IPL has 10 morphologically distinct sublaminae (Sanes & Zipursky 2010). In the inner six, rod and cone bipolar cells that depolarize to light increments (i.e., ON bipolar cells) stratify their axons, whereas the outer four are innervated by cone bipolar cells activated by light decrements (i.e., OFF bipolar cells). RGCs stratify their dendrites in cell type–specific patterns in the IPL to recruit excitatory and inhibitory input from unique combinations of bipolar and amacrine cells. These patterns of synaptic input combine with cell-intrinsic mechanisms to shape the feature preferences of RGCs.

RGCs innervate more than 50 areas of the mouse brain (Martersteck et al. 2017, Morin & Studholme 2014) (**Figure 2**). The dorsolateral geniculate nucleus (dLGN) of the thalamus passes information to the visual cortex and supports conscious visual perception (Kerschensteiner & Guido 2017, Liang & Chen 2020). The superior colliculus (SC) combines retinal signals with other sensory inputs to identify salient features and events in the environment, direct attention, and guide approach toward attractive stimuli and escape from threats (Cang et al. 2018, Dean et al. 1989, Krauzlis et al. 2013). In addition to these major retinorecipient targets innervated by most RGCs (Ellis et al. 2016, Román Rosón et al. 2019), a large number of brain areas receive type-restricted RGC input to mediate a wide range of behaviors and influences of light on physiology.

2. MOTION

Motion is one of the most common visual features that we experience. There are two primary sources of visual motion: movements of the observer (i.e., self-motion) and movements of objects in the observed world (i.e., object motion) (Frost 2010). In the retina, movements of the observer and objects cause global and local image motion, respectively. Motion-processing circuits in the retina either explicitly distinguish these forms of motion (e.g., object motion–sensitive circuits) or prefer local or global motion while selectively encoding other motion parameters [e.g., direction-selective (DS) circuits]. Finally, some retinal circuits respond strongly to objects approaching the observer (i.e., looming detection circuits) and initiate defensive responses to avoid collisions and evade predators.

2.1. Direction Selectivity

DS responses pervade the visual system. They help animals infer self-motion from optic flow and track moving objects. Motion direction is computed at multiple stages of the visual system, starting in the retina.

2.1.1. Direction-selective circuits and retinal ganglion cell types. DS RGCs were first discovered in rabbits (Barlow & Hill 1963, Barlow & Levick 1965, Barlow et al. 1964). The mouse retina dedicates approximately one-fifth of its output to signaling motion direction. The respective ganglion cells fall into two categories: ON DS RGCs, which respond to light increments, and ON-OFF DS RGCs, which respond to light increments and decrements (**Figure 3*a*,*b***). The presynaptic circuits of ON and ON-OFF DS RGCs overlap and compute motion direction by shared mechanisms, while unique mechanisms differentiate the speed and contrast preferences of ON and ON-OFF DS RGCs to match their behavioral functions (Mauss et al. 2017, Reinhard et al. 2020, Wei 2018).

At the core of retinal DS circuits, starburst amacrine cells (SACs) provide asymmetric inhibition to DS RGCs (ON SACs to ON DS RGCs and ON and OFF SACs to ON-OFF DS RGCs) (Briggman et al. 2011, Fried et al. 2002, Wei et al. 2011, Yonehara et al. 2011). SACs have radially symmetric dendrite arbors that receive input in their center and send output from their periphery (Briggman et al. 2011, Ding et al. 2016, Famiglietti 1991, Vlasits et al. 2016). Each primary SAC dendrite with its daughter branches functions as an independent motion sensor, preferring motion from the soma to the dendrite tips (Euler et al. 2002, Koren et al. 2017, Poleg-Polsky et al. 2018). This centrifugal motion preference arises from the passive membrane properties of SAC dendrites, their voltage-gated conductances, distributions of excitatory and inhibitory inputs, the dependence of excitatory input kinetics on distance from the soma, and SAC–SAC inhibition (Ding et al. 2016, Fransen & Borghuis 2017, Greene et al. 2016, Hausselt et al. 2007, Kim et al. 2014, Lee & Zhou 2006, Vlasits et al. 2016). Asymmetric connections of SACs with DS RGCs convert the SAC dendrites' centrifugal motion preferences into DS inhibition (Briggman et al. 2011); SAC dendrites pointing in the nasal direction form GABAergic synapses with DS RGCs that prefer temporal motion, whereas SAC dendrites pointing in the temporal direction form GABAergic synapses with nasal motion–preferring DS RGCs (Briggman et al. 2011). When SACs are silenced or killed, DS RGCs respond to motion in all directions (Pei et al. 2015, Vlasits et al. 2014, Yoshida et al. 2001), and increases and decreases in the SAC dendrites' retinal coverage sharpen and broaden DS RGC tuning, respectively (Morrie & Feller 2018, Soto et al. 2019). Thus, the subcellular computations of SAC dendrites and their asymmetric inhibitory connections determine the feature-selective output of DS RGCs.

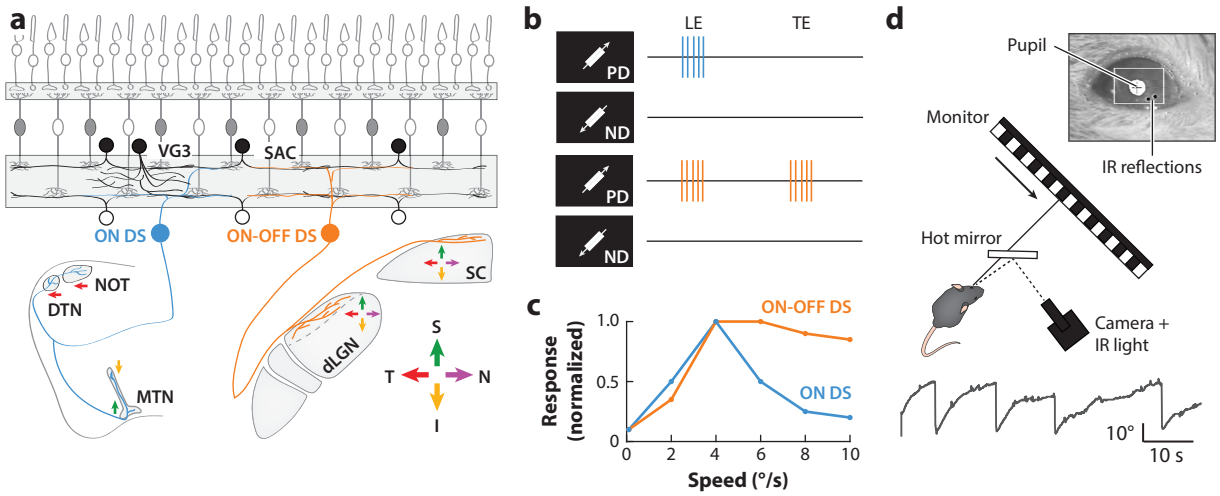

Figure 3

Direction-selective (DS) retinal ganglion cell (RGC) types, pathways, and functions. (*a*) ON and ON-OFF DS RGCs receive directionally selective inhibition from starburst amacrine cells (SACs). ON DS RGCs also receive input from VGLUT3-expressing (VG3) amacrine cells. ON DS RGCs preferentially innervate nuclei of the accessory optic system (AOS). Superior (S) and inferior (I) motion–preferring ON DS RGCs target the ventral and dorsal medial terminal nucleus (MTN), respectively. Temporal (T) [and potentially nasal (N)] motion–preferring ON DS RGCs target the nucleus of the optic tract (NOT) and dorsal terminal nucleus (DTN). ON-OFF DS RGCs of all direction preferences innervate the dorsolateral geniculate nucleus (dLGN) shell and the superior colliculus (SC). (*b*) Schematic of ON and ON-OFF DS RGC responses to bright bars moving in their preferred direction (PD) and opposite (i.e., null) direction (ND). ON DS RGCs respond to the leading edge (LE) of the stimulus only, whereas ON-OFF DS RGCs respond to the LE and the trailing edge (TE). (*c*) Responses of ON DS RGCs decline sharply with increasing stimulus speed, whereas ON-OFF DS RGCs signal motion direction over a wide range of speed. Tuning curves in this plot are estimated from Dhande et al. (2013). (*d*) Measurements of the optokinetic reflex driven by ON DS RGCs in head-fixed mice. Eye movements are measured by the differences in the position of the pupil relative to the reflections of an infrared (IR) light source. Panel *d* adapted with permission from Shen et al. (2020).

SACs are dual-transmitter neurons that release acetylcholine in addition to GABA (Lee et al. 2010). Cholinergic SAC–DS RGC connectivity is symmetric and supplements the excitatory drive from bipolar cells, particularly at low contrasts, to stabilize feature selectivity across lighting conditions (Lee et al. 2010, Pearson & Kerschensteiner 2015, Sethuramanujam et al. 2016, Yao et al. 2018).

In addition to GABAergic and cholinergic SAC input, ON-OFF DS RGCs receive glutamatergic input from bipolar cells. Two-photon calcium and glutamate imaging initially suggested that bipolar cell signals are not directionally tuned (Chen et al. 2014, Franke et al. 2017, Park et al. 2014, Yonehara et al. 2013). However, a recent study indicated that glutamate release from some boutons of type 2 (OFF) and type 7 (ON) bipolar cell axons, which synapse onto ON-OFF DS RGCs, may be DS (Matsumoto et al. 2020). This bouton-specific tuning relies on cholinergic and GABAergic modulation of bipolar cell axons by SACs (Matsumoto et al. 2020).

There are four ON-OFF DS RGC types in the mouse retina; they differ in their direction preferences (retinal direction: superior, inferior, nasal, and temporal) and gene expression and are labeled in different transgenic mouse lines (Bae et al. 2018, Elstrott et al. 2008, Fiscella et al. 2015, Huberman et al. 2009, Kay et al. 2011, Rivlin-Etzion et al. 2011, Sabbah et al. 2017, Tran et al. 2019, Trenholm et al. 2013). One of the four, the superior motion–preferring ON-OFF DS RGC, has asymmetric dendrite arbors that form gap junctions with same-type neighbors (Trenholm et al. 2013, 2014). This electrical coupling provides an anticipatory drive that counters the lag

between movement of stimuli and ganglion cell activation, bringing their positions into register (i.e., lag normalization) (Trenholm et al. 2013, 2014). Gap-junctional coupling also broadens the direction preferences of superior motion–preferring ON-OFF DS RGCs in dim light, favoring motion detection over directional precision (Yao et al. 2018). The behavioral significance of these adjustments and their restriction to a single ON-OFF DS RGC type remains to be determined.

ON-OFF DS RGCs are indirectly inhibited by wide-field amacrine cells, attenuating responses to global motion. Therefore, ON-OFF DS RGCs preferentially signal object motion direction, which they encode stably across a wide range of stimulus speeds (Hoggarth et al. 2015, Weng et al. 2005).

ON DS RGCs receive input from ON SACs, four ON bipolar cell types (5i, 5o, 5t, and 7), and VGLUT3-expressing (VG3) amacrine cells (Krishnaswamy et al. 2015, Lee et al. 2014, Matsumoto et al. 2019). Two-photon glutamate imaging and electron microscopic reconstructions suggest that the ON bipolar cell and VG3 amacrine cell inputs are arranged asymmetrically across ON DS RGC dendrites such that motion in the preferred direction activates slower inputs before faster ones, causing both slow and fast inputs to add up (Matsumoto et al. 2019). In contrast, motion in the opposite (i.e., null) direction elicits temporally dispersed excitation. Effective summation of excitation depends on the speed of preferred-direction motion. Thus, asymmetric excitation contributes to the ON DS RGCs' preference for slow stimulus speeds (Dhande et al. 2013, Gauvain & Murphy 2015, Matsumoto et al. 2019) (**Figure 3*c***).

Most studies have identified three ON DS RGC types that differ in their direction preferences (superior, inferior, and temporal), marker expression, and labeling in transgenic mouse lines (Dhande et al. 2013; Lilley et al. 2019; Martersteck et al. 2017; Yonehara et al. 2008, 2009). A recent study discovered a putative fourth, nasal motion–preferring ON DS RGC using large-scale two-photon calcium imaging (Sabbah et al. 2017). This study also revealed that the direction preferences of ON and ON-OFF DS RGCs vary across the retina to align with the optic flow fields generated by movements of mice forward and back and up and down (Sabbah et al. 2017).

In addition to ON and ON-OFF DS RGCs, DS responses have been reported for three RGC types with asymmetric dendrites (JAM-B, F-mini-ON, and F-mini-OFF RGCs) (Kim et al. 2008, Rousso et al. 2016). These RGC types are DS in specific stimulus conditions and robustly encode other visual features (Cooler & Schwartz 2020, Joesch & Meister 2016, Nath & Schwartz 2017). To what extent downstream pathways extract information about motion direction from JAM-B, F-mini-ON, and F-mini-OFF RGC inputs remains to be determined.

2.1.2. Downstream pathways and behavioral significance of retinal direction selectivity. DS RGCs differentially innervate three pathways (**Figure 3*a***). ON-OFF DS RGC axons preferentially target the dLGN of the thalamus and the SC, whereas ON DS RGC axons preferentially target nuclei of the accessory optic system (AOS). Recent studies have begun to uncover how downstream pathways process DS RGC inputs to guide behavior (Rasmussen & Yonehara 2020, Reinhard et al. 2020).

The dLGN passes signals from the retina to the primary visual cortex (V1) to support visual perception. The mouse dLGN is divided into a dorsolateral core and a ventromedial shell (Kerschensteiner & Guido 2017). ON-OFF DS RGCs predominantly innervate the dLGN shell (horizontal motion–preferring DS RGCs innervate the shell exclusively and vertical motion–preferring ON-OFF DS RGCs preferentially), while other RGCs innervate the dLGN core (Cruz-Martín et al. 2014, Hong et al. 2018, Huberman et al. 2009, Kay et al. 2011, Rivlin-Etzion et al. 2011). High-resolution functional imaging revealed that dLGN neurons in the shell receive input from DS RGC axons with similar or near-opposite direction preferences (Liang et al. 2018). This could, in principle, explain the abundant DS and motion axis–selective responses among

dLGN shell neurons (Liang et al. 2018, Marshel et al. 2012, Piscopo et al. 2013). Interestingly, in mice without horizontal motion–preferring DS RGCs, dLGN neuron preferences shift to vertical motion, but some horizontally DS responses persist (Rasmussen et al. 2020). Thus, direction selectivity in dLGN is partly inherited from the retina and partly generated by other mechanisms (e.g., computed in the dLGN or inherited from V1 or SC).

The axons of dLGN shell neurons innervate layer 2/3 of V1, whereas dLGN core neurons target V1's layer 4, continuing the parallel pathways from the retina (Cruz-Martín et al. 2014). Consistent with the preference of ON-OFF DS RGCs for the dLGN shell, perturbations of retinal direction selectivity disrupt responses in layer 2/3 but not layer 4, which generates DS responses from untuned dLGN inputs (Hillier et al. 2017, Lien & Scanziani 2018, Rasmussen et al. 2020). The deficits in layer 2/3 primarily affect high-speed posterior motion created when mice run forward (Hillier et al. 2017, Rasmussen et al. 2020). The behavioral significance of this ON-OFF DS RGC-dependent signal to cortical processing and behavior remains to be explored.

The SC integrates multisensory information, directs attention and orienting behaviors, and guides the pursuit of prey and escape from predators (Cang et al. 2018, Ito & Feldheim 2018). Most (85–90%) RGCs innervate the superficial SC (sSC) (Ellis et al. 2016, Hofbauer & Dräger 1985), and ON-OFF DS RGC axons stratify at the top of this retinorecipient zone (Huberman et al. 2009, Kay et al. 2011, Kim et al. 2010, Rivlin-Etzion et al. 2011). Many neurons near the surface of the SC are DS (de Malmazet et al. 2018, Inayat et al. 2015, Ito et al. 2017, Shi et al. 2017). Unlike the dLGN and V1, SC direction selectivity depends entirely on DS retinal input (Shi et al. 2017). Narrow-field cells are a genetically and morphologically distinct group of DS sSC neurons that project to the parabigeminal nucleus and deeper layers of the SC (Gale & Murphy 2014, Reinhard et al. 2019). Narrow-field neuron silencing impairs the ability of mice to detect and pursue prey (Hoy et al. 2019). Whether this contribution of narrow-field cells relies on their direction selectivity and if predator evasion or other SC-dependent behaviors are driven or modulated by ON-OFF DS RGC input remain to be tested.

A recent two-photon imaging study revealed that direction preferences in the SC are distributed inhomogeneously across visual space (de Malmazet et al. 2018). Specifically, SC neurons in the visual field's binocular area prefer nasal motion, whereas SC neurons in the monocular region prefer temporal motion (de Malmazet et al. 2018). This arrangement is well suited to distinguish optic flow from translations and rotations and may thus guide approach and escape behaviors.

Mice frequently move their eyes to compensate for head movements (Meyer et al. 2018, 2020; Michaiel et al. 2020). Two reflexes control gaze-stabilizing eye movements: the optokinetic reflex and the vestibulo-ocular reflex. The optokinetic reflex is driven by retinal image slip and operates at head-motion speeds too slow to activate the vestibular system (Faulstich et al. 2004) (**Figure 3*d***). The optokinetic reflex is mediated by the AOS, which encompasses the nucleus of the optic tract (NOT), the dorsal terminal nucleus (DTN), and the medial terminal nucleus (MTN) (Simpson 1984). ON DS RGCs dominate input to AOS nuclei (Dhande et al. 2013, Yonehara et al. 2009). Inferior and superior motion–preferring ON DS RGCs innervate the dorsal and ventral MTN, respectively, while nasal motion–preferring ON and ON-OFF DS RGCs innervate the NOT and DTN (Dhande et al. 2013; Kay et al. 2011; Yonehara et al. 2008, 2009) (**Figure 3*a***). Several lines of evidence suggest that DS RGC inputs to AOS nuclei drive gaze-stabilizing eye movements. First, SAC ablation or silencing abolishes the optokinetic reflex (Yoshida et al. 2001). Second, mutations of *Frmd7*, a common genetic cause of congenital nystagmus in humans (Tarpey et al. 2006), eliminate horizontal direction selectivity in the retina and the horizontal optokinetic reflex in mice and humans (Yonehara et al. 2016). Third, mutations that affect the connectivity of ON DS RGCs with AOS nuclei disrupt gaze-stabilizing eye movements (Osterhout et al. 2015,

Sun et al. 2015). The preference of ON DS RGCs for slow motion matches the speed tuning of the optokinetic reflex and complements the vestibulo-ocular reflex.

2.2. Object Motion Sensitivity

Object motion draws animals' attention (Kingdom & Prins 2016, Sillar et al. 2016). To reliably detect moving objects, retinal circuits need to distinguish local motion in a scene from global image motion caused by head and eye movements.

2.2.1. Object motion–sensitive circuits and retinal ganglion cell types. RGCs that distinguish local and global motion [i.e., object motion–sensitive (OMS) RGCs] were first identified in salamanders and rabbits (Baccus et al. 2008, Olveczky et al. 2003). Recently, a group of small OMS RGCs was identified in mice (Jacoby & Schwartz 2017, Zhang et al. 2012) (**Figure 4*a***). Based on transgenic labeling, Zhang et al. (2012) named one cell W3B (or W3), whereas Jacoby & Schwartz (2017) named four cells, based on morphology and resemblance to a famous rabbit RGC (Levick 1967, van Wyk et al. 2006), high-definition 1 (HD1), high-definition 2 (HD2), ultrahigh-definition (UHD), and local edge detector (LED) RGCs. It appears that UHD RGCs correspond to W3 RGCs (Schwartz & Swygart 2020). The four OMS RGCs' dendrites stratify in the middle of the IPL, where they receive input from rectified transient ON and OFF bipolar cells (Borghuis et al. 2013, Franke et al. 2017). This allows OMS RGCs to respond to local motion in their receptive field center, independent of the contrast composition (i.e., bright versus dark elements) of the moving object (Jacoby & Schwartz 2017, Zhang et al. 2012). In addition, OMS RGCs receive strong inhibition from their receptive field surrounds. Because this surround inhibition, like center excitation, is driven by rectified subunits, OMS RGCs are suppressed by

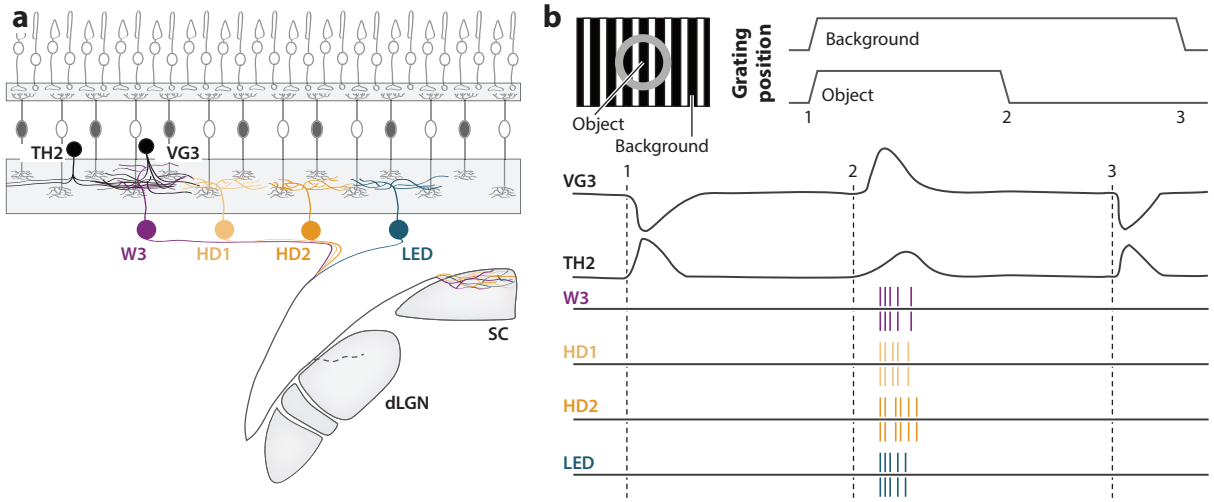

Figure 4

Object motion–sensitive (OMS) retinal ganglion cell (RGC) types, pathways, and functions. (*a*) Schematic of four small OMS RGCs identified in the mouse retina. W3 [or ultrahigh-definition (UHD)] RGCs receive excitatory input from VGLUT3-expressing (VG3) amacrine cells and inhibitory input from TH2 amacrine cells. OMS RGCs are underrepresented or absent from the dorsolateral geniculate nucleus (dLGN)-projecting set and strongly innervate the superior colliculus (SC). (*b*) VG3 amacrine cells distinguish local (2) and global (1) or surround (3) motion in their response polarity, whereas TH2 amacrine cells distinguish these stimuli in their response kinetics. All OMS RGCs respond strongly to isolated motion in their receptive field center, independent of the stimulus pattern, but are suppressed by simultaneous motion in the surround (i.e., global motion). Additional abbreviations: HD1, high-definition RGC type 1; HD2, high-definition RGC type 2; LED, local edge detector RGC.

global motion independent of the pattern of the shifting scene (Jacoby & Schwartz 2017, Zhang et al. 2012) (**Figure 4*b***). The four OMS RGC types prefer different motion speeds and delays between center and surround motion (Jacoby & Schwartz 2017), indicating that they may cooperate in signaling the speed of object motion relative to the observer.

Dissections of the composition and computations of W3 RGC circuits have provided interesting results. In addition to bipolar cells, W3 RGCs receive glutamatergic input from VG3 amacrine cells (Kim et al. 2015, Krishnaswamy et al. 2015, Lee et al. 2014). VG3 amacrine cells are themselves OMS and selectively amplify this feature in the W3 RGC response (Hsiang et al. 2017, Kim et al. 2015) (**Figure 4*b***). VG3 amacrine cells' dendrites are larger than those of bipolar cells but process inputs locally and, therefore, signal object motion with high spatial precision (Chen et al. 2017, Hsiang et al. 2017). The insertion of VG3 amacrine cells into the vertical pathway to W3 RGCs could delay excitation during motion in the receptive field center, allowing surround inhibition to cancel center excitation effectively during global image motion (Krishnaswamy et al. 2015) and/or enhance OMS responses by adding a layer of surround inhibition to the excitatory pathway (Kim & Kerschensteiner 2017, Kim et al. 2015).

W3 RGCs receive surround inhibition from TH2 amacrine cells (Brüggen et al. 2015, Kim & Kerschensteiner 2017, Knop et al. 2011), which respond to local and global motion but distinguish between these stimuli in their response kinetics (Kim & Kerschensteiner 2017) (**Figure 4*b***). Thus, global motion activates TH2 amacrine cells quickly, whereas local motion depolarizes them slowly. Slow depolarizations fail to elicit GABA release from TH2 amacrine cells, and differences in response kinetics are thus translated into global motion–selective inhibition of W3 RGCs (Kim & Kerschensteiner 2017). Thus, the OMS responses of W3 RGCs are shaped by the complementary actions of two amacrine cells. VG3 amacrine cells amplify responses to local motion, while TH2 amacrine cells suppress responses to global motion (Kim & Kerschensteiner 2017, Kim et al. 2015).

2.2.2. Downstream pathways and behavioral significance of retinal object motion sensitivity. Transgenic labeling revealed that W3 (UHD) RGC axons target the upper layer of the retinorecipient sSC (Zhang et al. 2012) (**Figure 4*a***). Disynaptic tracing showed that HD1 and HD2 RGCs innervate sSC neurons that send signals to the parabigeminal nucleus and the lateral posterior (LP) nucleus of the thalamus (i.e., the mouse pulvinar) (Reinhard et al. 2019). The targets of OMS RGCs in the sSC include wide-field cells, a genetically and morphologically distinct neuron type that innervates the LP nucleus of the thalamus (Gale & Murphy 2014). As their name suggests, wide-field neurons have large dendrites and correspondingly large receptive fields. However, they prefer motion of small objects anywhere within their receptive fields (Gale & Murphy 2014). Besides OMS RGC input, there are two key ingredients to the OMS responses of wide-field cells. First, dendritic spikes propagate signals elicited by object motion anywhere within their large dendritic arbors to the soma (Gale & Murphy 2016). Second, inhibitory inputs from sSC horizontal cells suppress responses to movements of large objects (Gale & Murphy 2016). Intriguingly, wide-field neuron silencing selectively impairs the mouse's ability to detect prey without affecting its pursuit (Hoy et al. 2019).

Retrograde labeling studies suggest that OMS RGCs are underrepresented in the dLGN-projecting set, indicating that among the two major retinorecipient targets, OMS RGCs preferentially innervate the SC (Ellis et al. 2016, Román Rosón et al. 2019) (**Figure 4*a***).

2.3. Looming Detection

Among object trajectories, a collision course with the observer is most alarming. Approaching objects cast expanding shadows (i.e., looming) that elicit innate defensive responses in most animals,

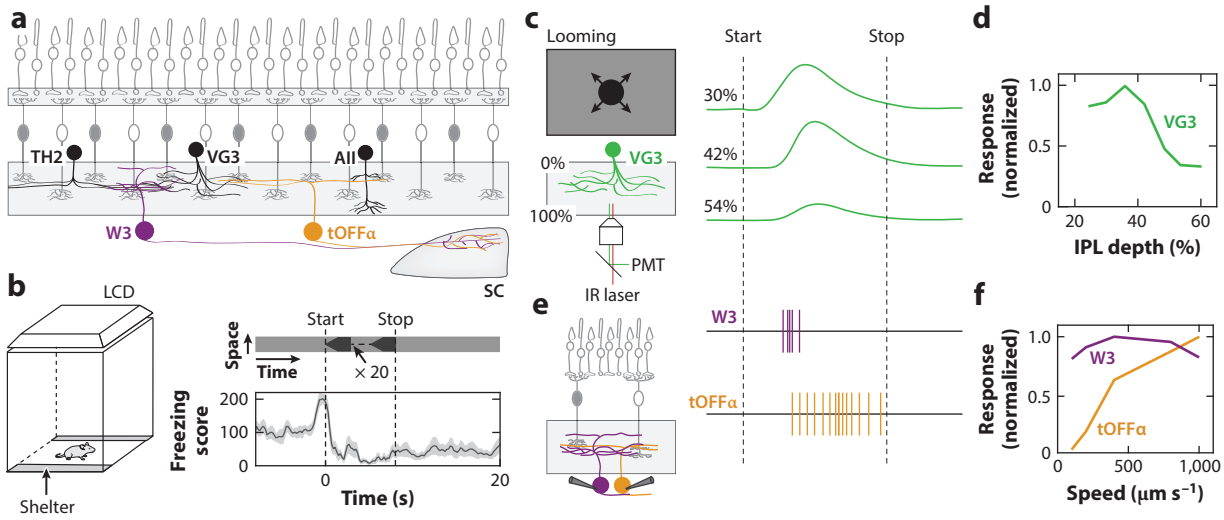

Figure 5

Looming detection and defensive behavior. (*a*) In looming detection circuits of the retina, VGLUT3-expressing (VG3) amacrine cells provide feature-selective excitatory input to W3 and tOFFα retinal ganglion cells (RGCs), which drive innate defensive responses through projections to the superior colliculus (SC). W3 RGCs combine this excitatory input with inhibition from TH2 amacrine cells, whereas tOFFα RGCs receive tonic inhibition from AII amacrine cells, which is relieved during looming. (*b*) Looming causes mice to flee to a virtual shelter and freeze (dashed lines indicate stimulus start and stop). (*c*) Two-photon calcium imaging of VG3 amacrine cell dendrites. (*d*) Looming responses are restricted to the proximal layers of the VG3 dendrite arbor. (*e*,*f*) By combining shared excitatory input with dissimilar inhibition, W3 and tOFFα RGCs encode the onset and speed of approach motion, respectively. Panels *b*–*f* adapted from Kim et al. (2020).

from insects to humans (Fotowat & Gabbiani 2011, Peek & Card 2016). Mice use vision to evade aerial predators (De Franceschi et al. 2016, Yilmaz & Meister 2013). Studies are beginning to elucidate the retinal circuits, RGC types, and downstream pathways that detect looming and drive innate defensive responses in mice.

2.3.1. Looming detection circuits and retinal ganglion cell types. Many RGCs respond to looming; fewer distinguish looming from related forms of motion (receding, white looming, etc.) (Münch et al. 2009, Reinhard et al. 2019). Knowing which retinal circuits drive innate defensive responses helps prioritize studies of looming processing. A recent study identified such a circuit in the mouse retina (Kim et al. 2020) (**Figure 5*a***). At the core of this circuit, VG3 amacrine cells, which receive input from ON and OFF bipolar cells, respond strongly to looming and weakly to related forms of motion. This preference arises from the stimulus-specific timing of excitation and inhibition. During looming, transient excitation precedes sustained inhibition, whereas excitation and inhibition coincide in response to expanding bright stimuli (Kim et al. 2020). The looming preferences of VG3 amacrine cells are enhanced by dendritic processing. Thus, looming-sensitive calcium transients in the VG3 dendrite arbor's proximal layer are segregated from weaker responses to related forms of motion in the distal dendrite layer (Kim et al. 2020) (**Figure 5*c*,*d***).

The proximal layer of the VG3 dendrite arbor provides glutamatergic input to two RGC types (W3 and tOFFα RGCs) that have been suggested to signal approaching aerial predators (Kim et al. 2015, 2020; Krishnaswamy et al. 2015; Lee et al. 2014; Münch et al. 2009; Zhang et al. 2012). W3 and tOFFα RGCs combine VG3 excitation with dissimilar inhibition to encode the onset (i.e., critical size) and speed of looming, respectively (**Figure 5*e*,*f***). During looming, W3 RGCs, like VG3

amacrine cells, receive transient excitation followed by sustained inhibition, in part from TH2 amacrine cells (Kim & Kerschensteiner 2017, Kim et al. 2020). This input sequence restricts W3 RGC responses to the onset of looming (critical size is approximately 4.5°). For stimuli expanding at different speeds, W3 RGC excitation and inhibition covary, keeping response amplitudes constant. Thus, W3 RGCs encode the onset (critical size) of looming independent of its speed (Kim et al. 2020). In contrast, tOFFα RGCs receive tonic inhibition, in part from AII amacrine cells, which is relieved by looming (Kim et al. 2020, Münch et al. 2009). Because excitation and disinhibition diverge as a function of stimulus speed, tOFFα RGC responses encode the speed of looming (Kim et al. 2020, Münch et al. 2009). The divergent feature representations of W3 and tOFFα RGCs resemble response types observed in looming-sensitive neurons in the pigeon tectum (equivalent to the SC of mice), indicating a conserved strategy in assessing predatory approaches (Sun & Frost 1998).

2.3.2. Downstream pathways and behavioral significance of retinal looming detection. Deletion of VG3 amacrine cells attenuates W3 and tOFFα RGCs' looming responses and diminishes defensive (flight and freeze) reactions to looming (Kim et al. 2020) (**Figure 5*b***). W3 and tOFFα RGCs innervate the sSC (Huberman et al. 2008, Reinhard et al. 2019, Zhang et al. 2012), which mediates defensive responses to visual threats (Blanchard et al. 1981, Dean et al. 1989, Sahibzada et al. 1986, Wei et al. 2015). On average, neurons in the sSC are innervated by six RGCs (Chandrasekaran et al. 2007). How input from W3, tOFFα, and other RGC types is combined to shape looming responses in the sSC remains to be explored. Neurons in the sSC respond robustly to looming (Lee et al. 2020, Reinhard et al. 2019, Zhao et al. 2014a). They inherit feature preferences from the retina, while input from V1 amplifies looming responses and enhances behavioral reactions to visual threats (Liang et al. 2015, Wang & Burkhalter 2013, Zhao et al. 2014a).

The responses of mice to looming depend on the environment and stimulus parameters. If shelters are available, then mice run to safety and freeze, even if threats are presented between them and the shelter (Vale et al. 2017, Yilmaz & Meister 2013). Escape delays depend on the stimulus salience (i.e., contrast) (Evans et al. 2018). Mice quickly learn the positions of shelters and update their escape behavior when shelters are moved (Vale et al. 2017). The shelter direction is conveyed continuously to the SC from the retrosplenial cortex and combined with threat assessments from the retina (Vale et al. 2020). When no shelters are available, mice freeze in place in response to looming (Vale et al. 2017, Wei et al. 2015, Yilmaz & Meister 2013), a behavior that is also elicited by sweeping visual stimuli (De Franceschi et al. 2016).

Looming signals of sSC neurons propagate along three pathways to shape defensive responses. First, sSC signals percolate to deeper layers of the SC (dSC). Compared to the sSC, dSC neurons are more selective for looming and depend less on stimulus positions, encode the behavioral salience (e.g., contrast) of the stimulus, and adapt quickly to repeated presentations (Evans et al. 2018, Lee et al. 2020). Neurons in the dSC innervate the dorsal periaqueductal gray with weak and unreliable excitatory connections that act as a threshold for escape initiation (Evans et al. 2018). dSC neurons also innervate GABAergic neurons in the ventral tegmental area, which respond to looming and inhibit the central amygdala (CeA). Inhibition of the CeA via this pathway promotes escape (Zhou et al. 2019). Second, sSC neurons provide input to the LP either directly or via the SC's intermediate layers. In turn, LP neurons send signals to the lateral amygdala (LA) (Wei et al. 2015). Optogenetic silencing and activation of neurons in these pathways prevent and promote freezing, respectively (Shang et al. 2018, Wei et al. 2015, Zingg et al. 2017). Third, sSC neurons innervate the parabigeminal nucleus (PBGN), which passes signals to the CeA (Shang et al. 2015). Optogenetic manipulations in this pathway suggest that it regulates escape responses

to visual threats, although the evidence is somewhat mixed (Evans et al. 2018; Shang et al. 2015, 2018; Zingg et al. 2017).

The sSC neurons that project to LP versus PBGN pathways receive input from overlapping but distinct RGC types (Reinhard et al. 2019). In addition, axon collaterals of one SC-projecting RGC type innervate GABAergic neurons in the dorsal raphe nucleus (DRN); these neurons inhibit their serotonergic DRN neighbors to promote escapes (Huang et al. 2017). In addition to understanding how different RGC types and different downstream pathways cooperate to initiate and guide defensive responses, determining where and how environmental factors and internal states intersect with visual signals to adapt behavioral responses to the animal's needs is an interesting area for future investigation (Evans et al. 2019).

3. ORIENTATION SELECTIVITY

Preferences for the orientation of static or moving stimuli (i.e., orientation selectivity) are prominent in the visual system, beginning in the retina. Different excitatory and inhibitory mechanisms give rise to orientation-selective (OS) responses of RGCs. Similar to DS RGCs, the contributions of OS RGCs to responses downstream are complex and target specific; their behavioral significance remains obscure.

3.1. Orientation-Selective Circuits and Retinal Ganglion Cell Types

OS RGCs were first identified in pigeons (Maturana & Frenk 1963) and rabbits (Levick 1967), where circuit mechanisms have been studied in some detail (Antinucci & Hindges 2018). More recently, robust OS responses were recorded in the mouse retina (Baden et al. 2016, Pearson & Kerschensteiner 2015, Zhao et al. 2013). Four morphologically and functionally distinct OS RGCs have been identified (Nath & Schwartz 2016, 2017) (**Figure 6*a***). Two OS RGCs prefer light increments (ON OS RGCs), and two prefer light decrements (OFF OS RGCs). In each category, one OS RGC prefers horizontal and the other vertical stimulus orientations (Nath & Schwartz 2016, 2017).

The excitation of ON OS RGCs is tuned to their preferred stimulus orientation, and their inhibition is orthogonally tuned (**Figure 6*b***). ON OS RGCs receive excitatory input from bipolar cells. Horizontal ON OS RGCs have horizontally elongated dendrite arbors and receive more bipolar cell input for stimuli aligned with their dendritic orientation (Nath & Schwartz 2016). In contrast, vertical ON OS RGCs have symmetric dendrite arbors, raising questions about their excitation tuning mechanisms. Because bipolar cells do not have oriented dendrites, one may speculate that presynaptic inhibition confers orientation selectivity to the output of some bipolar cell axons, similar to recent observations in DS circuits (Matsumoto et al. 2020). Orientation-tuned bipolar cell output has been observed in zebrafish but remains to be explored in the mouse retina (Johnston et al. 2019). Inhibition of vertical and horizontal ON OS RGCs is provided by OS GABAergic amacrine cells (Bloomfield 1994, Murphy-Baum & Taylor 2015, Nath & Schwartz 2016).

OFF OS RGCs combine orientation-tuned excitation and untuned inhibition (Nath & Schwartz 2017) (**Figure 6*b***). Intriguingly, rather than glutamatergic input from bipolar cells, gap-junctional input from OS amacrine cells with asymmetric dendrites drives OFF OS RGC responses (Nath & Schwartz 2017). Thus, OS amacrine cells are critical for the feature selectivity of ON (synaptic inhibition) and OFF (gap junctions) OS RGC responses. The identity of OS amacrine cells and how dendritic orientations and computations shape their feature preferences remain to be uncovered.

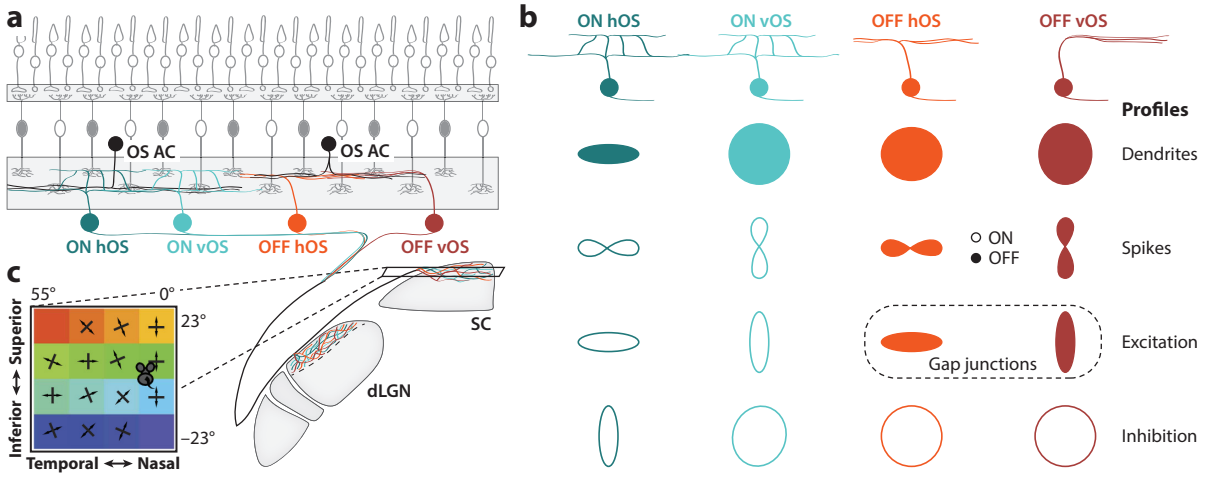

Figure 6

Orientation-selective (OS) retinal ganglion cell (RGC) types, pathways, and functions. (*a*) Four OS RGCs have been identified in mice; they respond to light increments (ON) or decrements (OFF) and one of two cardinal stimulus orientations [horizontal (hOS) and vertical (vOS)]. (*b*) Spatial profiles of dendrite, spike, excitatory, and inhibitory receptive fields of the four OS RGCs. The OS input to OFF OS RGCs is provided by gap junctions, likely with OS amacrine cells (ACs). Panel adapted with permission from Antinucci & Hindges (2018). (*c*) OS RGCs project to the dorsolateral geniculate nucleus (dLGN) shell and the superior colliculus (SC). Functional imaging of the sSC revealed that the orientation preferences of neurons are arranged concentrically around the center of the visual field. Panel adapted from Ahmadlou & Heimel (2015) (CC BY 4.0).

3.2. Downstream Pathways and Behavioral Significance of Retinal Orientation Selectivity

The vertical OFF OS RGC, also known as the JAM-B RGC, innervates the dLGN shell and the upper layer of the sSC (Kim et al. 2008, Nath & Schwartz 2017) (**Figure 6*c***). OS responses have been recorded in both targets (Marshel et al. 2012, Piscopo et al. 2013, Scholl et al. 2013, Wang et al. 2010, Zhao et al. 2013).

In the dLGN, OS (or motion axis–selective) responses are restricted to the shell (Marshel et al. 2012, Piscopo et al. 2013) and are partially inherited from OS RGCs and partially constructed by combining input from DS RGCs with opposite direction preferences (Liang et al. 2018). Restriction to the shell suggests that OS signals from the retina and dLGN reach the superficial layers of V1 through a distinct channel, similar to DS signals (Cruz-Martín et al. 2014). The contribution of this channel to cortical processing and its behavioral purpose remains to be elucidated. Independently, V1 layer 4 neurons derive OS responses from untuned dLGN inputs, as originally proposed by Hubel & Wiesel (1962; see also Lien & Scanziani 2013).

Approximately 20% of sSC neurons are OS (de Malmazet et al. 2018, Wang et al. 2010). In vivo two-photon imaging revealed that the orientation preferences of sSC neurons are organized into columns (Ahmadlou & Heimel 2015, Feinberg & Meister 2015). Neurons within each column prefer the same stimulus orientation throughout the depth of the sSC. Surprisingly, adjacent columns not only differ in their orientation preferences, but also cover different areas of visual space (Ahmadlou & Heimel 2015, Feinberg & Meister 2015). Consequently, orientation preferences are distributed inhomogeneously across visual space with gaps in coverage (Ahmadlou & Heimel 2015, de Malmazet et al. 2018, Feinberg & Meister 2015). Intriguingly, sSC columns in the binocular part of the mouse visual field prefer horizontal stimulus orientations, whereas sSC columns in the monocular part are concentrically arranged in visual space (Ahmadlou & Heimel

2015, de Malmazet et al. 2018) (**Figure 6*c***). The behavioral significance of this arrangement and its interactions with the independent direction selectivity maps of the SC remain to be uncovered.

4. LUMINANCE CONTRAST

Spatiotemporal variations in brightness (i.e., luminance contrast) are a fundamental feature of visual scenes and shape our perception of the world (Delorme et al. 2000, Kaplan 2008, Stone et al. 1990). Most RGCs, including those with higher-order feature selectivities, are activated by simple luminance contrast stimuli (e.g., flashing bright or dark spots). Yet, from rodents to primates, one RGC class is active in featureless environments and suppressed by contrast.

4.1. Contrast Detection

The orthodox view of RGC function is that their center-surround receptive fields extract local luminance contrast (Kuffler 1953). However, even among the more conventional mouse RGC types, recent studies have identified diverse receptive field architectures and synaptic mechanisms that differentiate contrast preferences to fit behavioral demands that remain to be fully understood.

4.1.1. Contrast detection circuits and retinal ganglion cell types. This section reviews three groups of contrast-encoding mouse RGCs: α RGCs, Pix_{ON} RGCs, and F RGCs (**Figure 7*a***). When targeting large cell bodies in the ganglion cell layer of the mouse retina, one consistently records three RGC types: one with sustained ON responses, one with sustained OFF responses, and one with transient OFF responses (Margolis & Detwiler 2007, Murphy & Rieke 2006, Pang et al. 2003). Based on morphological similarities to cat RGCs, these cells are called α RGCs (Boycott & Wässle 1974, Pang et al. 2003, Sun et al. 2002). Sustained ONα (sONα) and sustained OFFα (sOFFα) RGCs form a paramorphic pair (i.e., ON and OFF versions of a morphological type), possibly homologous to α (-like) RGC pairs in other rodents, cats, nonhuman primates, and humans (Boycott & Wässle 1974, Dacey & Petersen 1992, Peichl et al. 1987, Soto et al. 2020, Vitek et al. 1985).

Despite their paramorphy, sONα and sOFFα differ functionally beyond their preference for ON versus OFF stimuli. sONα and sOFFα RGCs exemplify two canonical arrangements of excitatory and inhibitory receptive fields (**Figure 7*a***). sONα RGCs receive excitation from ON bipolar cells and inhibition from amacrine cells driven by the same bipolar cells (i.e., ON amacrine cells) (Morgan et al. 2011, Park et al. 2018, Schwartz et al. 2012). In this feedforward circuit, sONα RGCs' firing to temporal contrast is driven by excitation (Murphy & Rieke 2006). Type 6 bipolar cells account for approximately 70% of the excitatory input to sONα RGCs (Morgan et al. 2011, Schwartz et al. 2012, Tien et al. 2017). Tonic glutamate release from type 6 bipolar cells contributes to the high firing rates of sONα RGCs at the mean light level in an environment and their exquisite sensitivity to small fluctuations around the mean (i.e., high contrast sensitivity) (Sabbah et al. 2018, Schwartz et al. 2012, Zaghloul et al. 2003). Interestingly, sONα RGCs can substitute B6 cells with a type-specific complement of other bipolar cells to preserve their high contrast sensitivity and linear response functions when B6 cells are ablated during development (Tien et al. 2017).

In contrast, sOFFα RGCs receive excitation from OFF bipolar cells—including a unique dendriteless type—and inhibition from ON amacrine cells (Della Santina et al. 2016, Murphy & Rieke 2006, Pang et al. 2003). In this push–pull circuit, the firing of sOFFα RGCs to temporal contrast is driven by the coincidence of excitation and disinhibition (Murphy & Rieke 2006).

In addition to differences in temporal contrast processing, sONα and sOFFα RGCs integrate spatial contrast differently. The nonlinear subunits of sONα RGC receptive fields allow them to

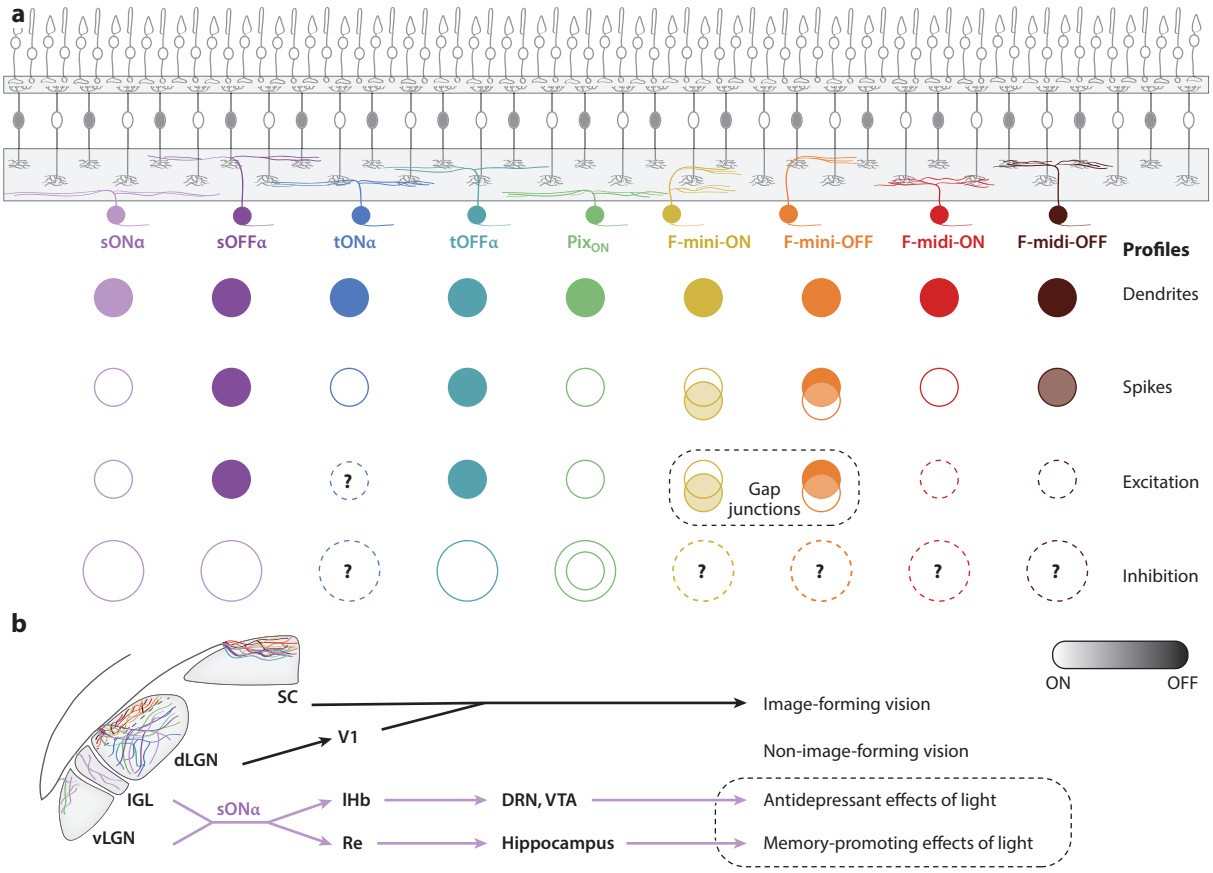

Figure 7

Contrast-encoding α, Pix$_{ON}$, and F retinal ganglion cells (RGCs), pathways, and functions. (*a*) Schematic of four α RGCs (sONα, sOFFα, tONα, tOFFα), the Pix$_{ON}$ RGC, and four F RGCs (F-mini-ON, F-mini-OFF, F-midi-ON, F-midi-OFF) and the spatial profiles of their dendrites and spike, excitatory, and inhibitory receptive fields. (*b*) α and Pix$_{ON}$ RGCs project to the dorsolateral geniculate nucleus (dLGN) core, whereas F RGCs project to the dLGN shell. Projections to the dLGN and superior colliculus (SC) mediate image-forming functions of vision. In addition, sONα RGCs densely innervate the ventrolateral geniculate nucleus (vLGN) and intergeniculate leaflet (IGL) to mediate non-image-forming functions. Additional abbreviations: 1Hb, lateral habenula; DRN, dorsal raphe nucleus; Re, nucleus reuniens; V1, primary visual cortex; VTA, ventral tegmental area.

respond to luminance-invariant changes in stimulus patterns (i.e., nonlinear spatial integration), whereas sOFFα RGCs sum stimulus intensity across their receptive fields and respond only if the result changes (i.e., linear spatial integration) (Krieger et al. 2017, Schwartz et al. 2012). In addition to extending response functions to higher spatial frequencies (i.e., finer spatial detail), nonlinear interactions of bipolar cells, which comprise the receptive field subunits, sensitize sONα RGCs to motion (Kuo et al. 2016). In dim light, the spatial integration of sONα RGCs becomes linear, as the membrane potential of the bipolar cells depolarizes to a linear input–output range (Grimes et al. 2014). This switch to linear integration may average out noise from quantal fluctuations in photon absorption and preserve contrast sensitivity at the expense of fine spatial detail in dim light (Grimes et al. 2014).

Finally, sONα but not sOFFα RGCs encode luminance (Schmidt et al. 2014, Sonoda et al. 2018). The luminance encoding of sONα RGCs depends on their expression of the photopigment

melanopsin—sONα RGCs are, therefore, also known as M4 intrinsically photosensitive RGCs (ipRGCs) (Ecker et al. 2010). Melanopsin mediates only small photocurrents in sONα RGCs, but second messengers close potassium channels to increase sONα RGC excitability and firing rates in a light-dependent manner (Ecker et al. 2010, Jiang et al. 2018, Schmidt et al. 2014, Sonoda et al. 2018). It has been suggested that bipolar cells also contribute to the luminance encoding of sONα RGCs (Sabbah et al. 2018).

Transient OFFα (tOFFα) RGCs combine OFF excitation with ON inhibition (i.e., push–pull circuit), and their firing to temporal contrast relies on coincident excitation and disinhibition (Murphy & Rieke 2006, Pang et al. 2003) (**Figure 7*a***). As discussed in Section 2.3, VG3 amacrine cells contribute to the excitation of tOFFα RGCs, and AII amacrine cells contribute to their tonic inhibition (Kim et al. 2020, Krishnaswamy et al. 2015, Lee et al. 2014, Münch et al. 2009). tOFFα RGCs integrate spatial information nonlinearly and are highly sensitive to motion, particularly approach motion (Kim et al. 2020, Krieger et al. 2017, Münch et al. 2009). In addition, tOFFα RGCs receive gap-junctional input, which increases their sensitivity to dim light flashes (Murphy & Rieke 2011).

Recent studies identified a putative paramorphic partner of transient tOFFα RGCs. tONα RGCs are labeled with the other α RGCs in *Kcgn4-Cre* transgenic mice; express the group-specific markers SMI32 and SPP1; cluster with the other α RGCs in transcriptomic analyses; and, like the other α RGCs, have narrow action potentials (Krieger et al. 2017, Tran et al. 2019). tONα RGCs integrate spatial information nonlinearly. The stimulus preferences of tONα RGCs and underlying circuit mechanisms remain to be studied in more detail.

In primates, midget RGCs mediate high-acuity vision. The simple preferences of midget RGCs, particularly in the fovea, resemble photoreceptor pixel representations (Sinha et al. 2017). A recent study identified a pixel-encoder RGC type (Pix_{ON} RGCs) with noncanonical receptive fields in mice (Johnson et al. 2018) (**Figure 7*a***). Pix_{ON} RGCs receive only excitatory input (from ON bipolar cells) for stimuli overlaying their dendrites and only inhibitory input (from ON amacrine cells) for stimuli outside of their dendrite arbors (Johnson et al. 2018). Excitatory inputs to Pix_{ON} RGCs integrate spatial information linearly, and, because of tonic excitation and high baseline firing rates, Pix_{ON} RGCs signal increases and decreases in stimulus intensity approximately linearly (Johnson et al. 2018). The exclusion of inhibition from the receptive field center increases the gain of excitation-to-spike conversion. The truly lateral inhibition from the donut-shaped inhibitory receptive fields is provided by spiking GABAergic amacrine cells and is temporally matched to excitation, simplifying the contrast encoding of Pix_{ON} RGCs and enhancing the representation of edges in a scene (Johnson et al. 2018).

An analysis of transcription factor profiles revealed that approximately 20% of RGCs express the forkhead/winged-helix domain protein FOXP2 (i.e., F RGCs) (Rousso et al. 2016). The F RGC family has four members comprising two paramorphic pairs named for their arbor size and contrast preferences, F-midi-ON and F-midi-OFF and F-mini-ON and F-mini-OFF (Rousso et al. 2016) (**Figure 7*a***). The four F RGCs coexpress unique combinations of FOXP1 and BRN3a-c with FOXP2, suggesting that a combinatorial transcription factor code drives their differentiation (Rousso et al. 2016). F-midi-ON cells respond exclusively to light increments, F-midi-OFF cells respond more robustly to light decrements, and both F-midi-ON and F-midi-OFF cells prefer small stimuli (Rousso et al. 2016). Other stimulus preferences and the underlying circuit mechanisms remain to be uncovered.

F-mini-ON and F-mini-OFF RGCs are the second and third most abundant RGC types in the mouse retina, respectively, and account for 13% of all RGCs (Rousso et al. 2016). Despite differences in their dendritic stratification, both F-mini-ON (bistratified) and F-mini-OFF

(monostratified) RGCs respond to light increments and decrements (Cooler & Schwartz 2020). Intriguingly, the ON and OFF receptive fields of F-mini-ON RGCs are consistently offset, with OFF fields offset 30–40 μm ventrally from ON fields (Cooler & Schwartz 2020). Rather than glutamate release from OFF bipolar cells, gap-junctional coupling to F-mini-OFF RGCs delivers OFF excitation to F-mini-ON RGCs and vice versa (Cooler & Schwartz 2020). On average, four F-mini-OFF RGCs are coupled to each F-mini-ON RGC, and approximately four F-mini-ON RGCs are coupled to each F-mini-OFF RGC. In conjunction with dendritic asymmetries, this unexpected consummation of their paramorphic pairing accounts for the offset between the ON and OFF receptive field of F-mini-ON and F-mini-OFF RGCs, which modeling suggests increases the precision of edge detection in the retina (Cooler & Schwartz 2020).

4.1.2. Downstream pathways and behavioral significance of retinal contrast detection. Although projection patterns remain to be mapped comprehensively and cell type specifically, transgenic labeling and retrograde tracing revealed that α RGCs, Pix_{ON} RGCs, and F RGCs target the dLGN (Ecker et al. 2010, Ellis et al. 2016, Huberman et al. 2008, Johnson et al. 2018, Martersteck et al. 2017, Román Rosón et al. 2019, Rompani et al. 2017, Rousso et al. 2016) (**Figure 7*b***). α RGCs and Pix_{ON} RGCs innervate the dLGN core, and F RGCs innervate the dLGN shell, indicating that they provide input to parallel pathways from the retina to V1 (Cruz-Martín et al. 2014, Ecker et al. 2010, Huberman et al. 2008, Johnson et al. 2018, Martersteck et al. 2017, Rompani et al. 2017, Rousso et al. 2016).

The convergence of RGC axons onto thalamocortical (TC) projection neurons in the dLGN has been analyzed extensively (Liang & Chen 2020). Recent anatomical and functional evidence indicates that 10 or more RGCs converge onto each TC neuron, but a few dominate its responses (Hammer et al. 2015, Litvina & Chen 2017, Morgan et al. 2016, Rompani et al. 2017). Different modes of functional convergence can be distinguished. Whereas some TC neurons combine input from a single or functionally similar RGC type(s) (i.e., relay mode), others combine input from RGCs with different feature preferences (i.e., combination mode) (Liang et al. 2018, Rompani et al. 2017). α RGCs and Pix_{ON} RGCs are overrepresented in the dLGN-projecting set and contribute to relay-mode and combination-mode convergence, which preserves and transforms, respectively, the RGCs' responses on the way to V1 (Piscopo et al. 2013, Román Rosón et al. 2019, Rompani et al. 2017, Suresh et al. 2016). TC neurons of the dLGN core project to layer 4 of V1. Precise spatial offsets of approximately 80 converging ON and OFF TC neurons generate OS responses in V1 layer 4 neurons, and spatial offsets combine with temporal mismatches (i.e., transient-sustained, sustained-transient) of ON and OFF TC neurons to generate DS responses (Lien & Scanziani 2013, 2018; Liu et al. 2010).

A recent study found that sONα RGCs determine the perceptual threshold for dim light detection in mice, likely through signals propagating along the retino-geniculo-cortical pathway (Smeds et al. 2019).

Axon collaterals of α RGCs, Pix_{ON} RGCs, and F RGCs innervate the sSC (Ecker et al. 2010, Ellis et al. 2016, Hong et al. 2011, Huberman et al. 2009, Johnson et al. 2018, Martersteck et al. 2017, Rousso et al. 2016) (**Figure 7*b***). Functional evidence indicates that approximately six RGCs converge onto each sSC neuron (Chandrasekaran et al. 2007). Unlike TC neurons (Grubb & Thompson 2003), most sSC neurons combine inputs from ON and OFF responsive RGCs (Wang et al. 2010). Recently, Reinhard et al. (2019) analyzed the RGC complements that provide input via the sSC to the PBGN and LP. They found that sOFFα, tOFFα, tONα, Pix_{ON}, F-mini-ON, and F-midi-ON RGCs distribute input evenly between both pathways. In contrast, sONα RGCs send signals preferentially to the PBGN, F-mini-OFF RGCs send signals preferentially to the

LP, and F-midi-OFF RGCs send signals to neither (Reinhard et al. 2019). These distinct RGC complements' contributions to feature representations along these pathways and behavior remain to be uncovered.

Recently, sONα RGCs were found to dominate input to two pathways through the ventrolateral geniculate nucleus (vLGN) and intergeniculate leaflet (IGL), which, together with the dLGN, make up the LGN complex (Monavarfeshani et al. 2017) (**Figure 7*b***). First, sONα RGCs innervate GABAergic neurons in the vLGN and IGL that project to the lateral habenula (LHb) and mediate antidepressant effects of light (Huang et al. 2019). Second, sONα RGCs innervate CaMKIIα neurons in the vLGN and IGL, which provide a mixture of excitation and inhibition to the nucleus reuniens (Re) to promote spatial memory formation (Huang et al. 2021). Antidepressant and memory-promoting effects are thought to rely on luminance rather than contrast signals. How parallel pathways through the LGN complex extract different information from the sONα RGC inputs (the dLGN extracting contrast information and the vLGN and IGL extracting luminance information) is a fundamental open question.

4.2. Suppressed-by-Contrast Signals

All of the RGCs discussed above fire action potentials to signal positive contrast features (ON), negative contrast features (OFF), or both (ON-OFF). However, one conserved RGC class is active in featureless environments and silenced by contrast.

4.2.1. Suppressed-by-contrast circuits and retinal ganglion cell types. Suppressed-by-contrast (SbC) RGCs were first discovered in rabbits and cats (Levick 1967, Rodieck 1967) and later identified in nonhuman primates (de Monasterio 1978). Because they prefer featureless environments, SbC RGCs have also been called uniformity detectors (Levick 1967, Sivyer & Vaney 2010, Sivyer et al. 2010). Recently, two groups characterized SbC RGCs with different suppression kinetics in mice (Jacoby et al. 2015, Tien et al. 2015) (**Figure 8*a*,*b***). Transient SbC (tSbC) RGCs stop firing for approximately 0.5 s after light increments or decrements (Tien et al. 2015), whereas sustained SbC (sSbC) RGCs are silenced for the duration of light steps (up to 20 s) (Jacoby et al. 2015). tSbC RGCs have also been described as delayed ON RGCs because their firing rates can rebound above baseline after light increments transiently suppress them (Jacoby & Schwartz 2018, Mani & Schwartz 2017). Both tSbC and sSbC RGCs have bistratified

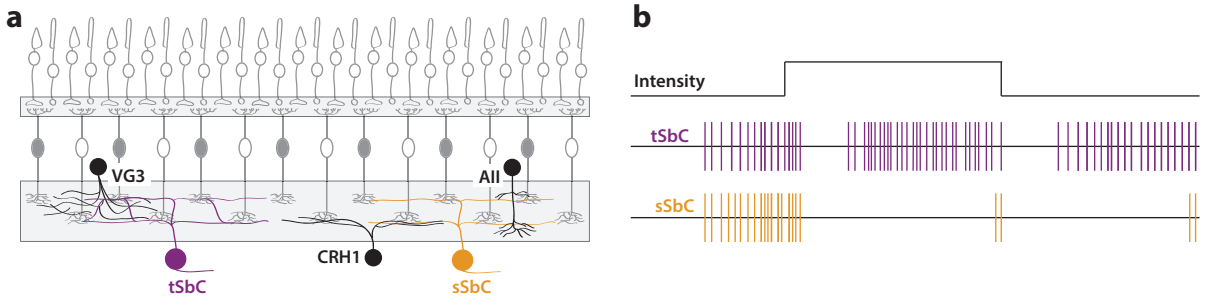

Figure 8

Suppressed-by-contrast RGC types. (*a*) Schematic illustration of tSbC and sSbC RGCs and the presynaptic amacrine cell types that shape the suppressive contrast encoding. (*b*) Schematic of transient and sustained spike suppression light increments and decrements in tSbC and sSbC RGCs, respectively. Abbreviations: AII, amacrine cell; CRH1, corticotropin-releasing hormone-expressing amacrine cell type 1; RGC, retinal ganglion cell; sSbC, sustained suppressed-by-contrast; tSbC, transient suppressed-by-contrast; VG3, VGLUT3-expressing amacrine cell.

dendrites but receive glutamatergic input only from ON bipolar cells (Jacoby et al. 2015, Tien et al. 2015). ON excitation is weak and overwhelmed by ON inhibition, whereas suppression of tonic excitation coincides with inhibition at light OFF (Jacoby et al. 2015, Tien et al. 2015). The arbors of tSbC RGCs have frequent recursions in which dendrites from the OFF layer dive back to the ON layer and ON dendrites ascent to the OFF layer far from the soma (Ivanova et al. 2013, Tien et al. 2015, Zhu et al. 2014). Recursive dendrite arbors are also a hallmark of SbC RGCs in rabbits (Sivyer & Vaney 2010).

Inhibition kinetics differentiate the suppressive responses of tSbC and sSbC RGCs. tSbC RGCs receive transient, predominantly glycinergic inhibition at light ON and OFF (Tien et al. 2015). Optogenetic and anatomical circuit mapping identified VG3 amacrine cells as a source of tSbC RGC inhibition (Lee et al. 2016, Tien et al. 2016). This, in turn, identified VG3 amacrine cells as dual transmitter neurons, which use their two transmitters (glutamate and glycine) in a target-specific manner (Lee et al. 2016, Tien et al. 2016). Interestingly, the transient VG3 amacrine cells preferentially synapse onto the ascending and descending processes of tSbC dendrites, providing a functional explanation for this conserved morphological feature (Tien et al. 2016). Type-specific cell deletion showed that VG3 amacrine cells silence tSbC RGCs in response to small OFF stimuli (Tien et al. 2016). The amacrine cells that inhibit tSbC RGCs in response to ON and large OFF stimuli remain to be identified. In contrast, sSbC RGCs receive sustained predominantly GABAergic inhibition at light ON and OFF (Jacoby et al. 2015). Paired recordings and type-specific cell ablation demonstrated that CRH-1 amacrine cells are the source of sustained ON inhibition to sSbC RGCs (Jacoby et al. 2015). The amacrine cells that inhibit sSbC RGCs in response to OFF stimuli remain to be identified. Thus, tSbC and sSbC RGCs illustrate how specific amacrine cell combinations shape the feature representations of the retinal output. The modularity of interneuron circuits in the retina may be replicated in other parts of the nervous system.

4.2.2. Downstream pathways and behavioral significance of retinal suppressed-by-contrast signals. The projection patterns of tSbC RGCs and sSbC RGCs remain to be analyzed in detail, but recent retrograde labeling experiments indicated that SbC-responsive cells abound among the dLGN-projecting RGCs (Román Rosón et al. 2019). SbC responses have also been recorded in the dLGN and V1 of mice and nonhuman primates (Niell & Stryker 2010, Piscopo et al. 2013, Zeater et al. 2015), suggesting that tSbC and sSbC RGC signals may propagate along dedicated pathways from the retina to the cortex. In addition, SbC responses could arise independently at subsequent stages of the retino-geniculo-cortical pathway, analogous to OS and DS responses (Niell 2013). SbC RGC inputs also converge with conventional RGC inputs in the dLGN (Liang et al. 2018). The function of SbC signals, which have also been recorded in the SC, remains mysterious (Ito et al. 2017, Masland & Martin 2007). Current hypotheses range from contrast gain control of conventional signals to detection of self-generated visual stimuli (e.g., eye movements and blinks) (Masland & Martin 2007, Tailby et al. 2007, Tien et al. 2015).

4.3. Luminance Encoding

Ambient light levels influence a wide range of physiological processes and behaviors (i.e., non-image-forming vision). The persistence of these influences (e.g., circadian photoentrainment and suppression of melatonin) in patients and mice without rods and cones, and the loss of these influences in enucleated mice and *Math5* mutants, which lack signals from the eye to the brain, suggested the existence of another photoreceptive neuron in the retina (Brzezinski et al. 2005, Czeisler et al. 1995, Ebihara & Tsuji 1980, Freedman et al. 1999, Lucas et al. 1999, Wee et al. 2002, Zaidi et al. 2007).

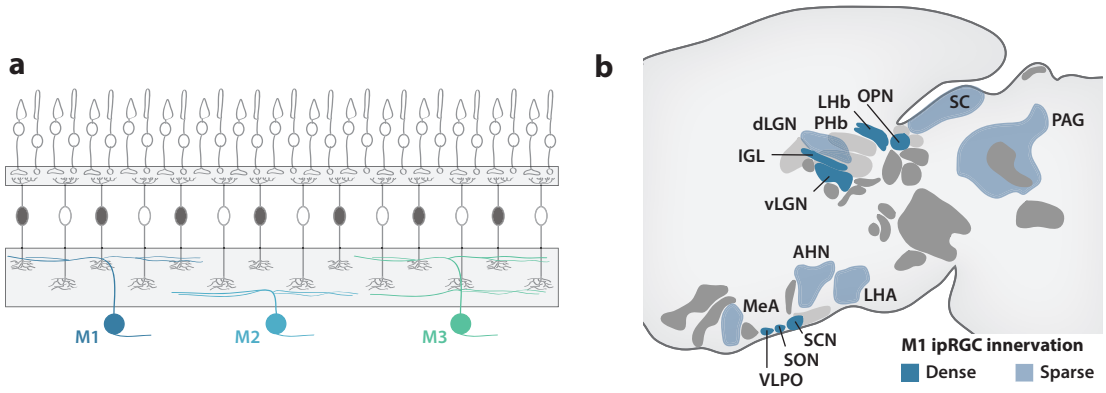

Figure 9

Melanopsin-expressing RGC types and pathways. (*a*) Schematic illustration of M1–M3 ipRGCs. (*b*) M1 ipRGCs send luminance signals to a wide range of brain areas that mediate image-forming and non-image-forming functions. Abbreviations: AHN, anterior hypothalamic area; dLGN, dorsolateral geniculate nucleus; IGL, intergeniculate leaflet; ipRGC, intrinsically photosensitive RGC; LHA, lateral hypothalamic area; LHb, lateral habenula; MeA, medial amygdala, anterior; OPN, olivary pretectal nucleus; PAG, periaqueductal gray; PHb, perihabenular nucleus; RGC, retinal ganglion cell; SC, superior colliculus; SCN, suprachiasmatic nucleus; SON, supraoptic nucleus; vLGN, ventrolateral geniculate nucleus; VLPO, ventrolateral preoptic area.

4.3.1. Luminance-encoding circuits and retinal ganglion cell types. Through retrograde tracing from the suprachiasmatic nucleus (SCN), the source of circadian rhythms and the site of their photoentrainment, Berson et al. (2002) discovered RGCs that remained light sensitive when pharmacologically or physically removed from the retina. Hattar et al. (2002) demonstrated that these ipRGCs express melanopsin, a photopigment previously identified in the retina (Provencio et al. 1998, 2000), and project to brain areas involved in non-image-forming vision. Since then, several melanopsin-expressing (M) ipRGC types have been distinguished in mice, and their contributions to physiology and behavior are being deciphered. The ipRGCs have been reviewed comprehensively elsewhere (Aranda & Schmidt 2020, Do 2019, Do & Yau 2010, Lazzerini Ospri et al. 2017, Van Gelder & Buhr 2016). In this section, I highlight recent advances in our understanding of ipRGC diversity and the downstream pathways through which they shape physiology and behavior.

The count of ipRGC types is up to six (M1–M6) (**Figure 9*a***). The M1 ipRGCs initially identified by Berson et al. (2002) have the largest intrinsic photocurrents and signal changes in average luminance, with little response to transient or local fluctuations in light intensity (i.e., contrast) (Ecker et al. 2010, Zhao et al. 2014b). By comparison, M2–M6 ipRGCs have small intrinsic photocurrents. Driven by synaptic inputs, the spike trains of M2–M6 ipRGCs encode contrast (Ecker et al. 2010, Quattrochi et al. 2018, Zhao et al. 2014b). In addition, the average firing rates of M2–M4 ipRGCs signal average luminance (Ecker et al. 2010, Zhao et al. 2014b). To what extent this luminance signal reflects sustained excitatory synaptic inputs, intrinsic photocurrents, and melanopsin's influences on excitability remains to be determined (Ecker et al. 2010, Sabbah et al. 2018, Sonoda et al. 2018, Zhao et al. 2014b). In M4 ipRGCs (also known as sONα RGCs), second-messenger signals from melanopsin close potassium channels, increasing input resistance and the impact of synaptic excitation (Sonoda et al. 2018). Thus, increases in luminance raise the contrast sensitivity of M4 ipRGCs, highlighting the importance of understanding the interactions of intrinsic and synaptic signals in ipRGCs (Sonoda et al. 2018). Luminance encoding of M5 ipRGC (also known as Pix_{ON} RGCs) has not been explored (Johnson et al. 2018, Stabio et al. 2017), and M6 ipRGCs appear not to signal luminance (Levine & Schwartz 2020).

The dendrites of M1–M6 ipRGCs stratify in different patterns. M1 dendrites stratify in the IPL's OFF sublamina; M2, M4, and M5 dendrites stratify in the ON sublamina; and M3 and M6 dendrites are bistratified, targeting the ON and OFF sublamina. Despite differences in stratification, the dendrites of all ipRGC types receive glutamatergic input exclusively from ON bipolar cells (Ecker et al. 2010, Quattrochi et al. 2018, Zhao et al. 2014b). M1 dendrites recruit ON bipolar cell inputs from axons passing through the IPL's OFF layer (Dumitrescu et al. 2009, Hoshi et al. 2009). The vast majority (approximately 95%) of en-passant synapses are formed by type 6 bipolar cells and differ ultrastructurally from their terminal synapses (Sabbah et al. 2018). The purpose of this arrangement and functional consequences of the en-passant synapse ultrastructure remain to be uncovered.

Luminance varies by $>10^9$ from moonless nights to sunny days (Rieke & Rudd 2009). Encoding this vast brightness range with a single neuron type could result in poor luminance resolution. However, recent studies revealed that M1 ipRGCs divide the light intensity range among themselves to encode luminance accurately as a population (Milner & Do 2017) and identified mechanisms underlying this population coding (Emanuel et al. 2017, Lee et al. 2019). Milner & Do (2017) discovered that most M1 ipRGCs have nonmonotonic intensity-response functions, in which firing rates rise from darkness to a preferred-luminance peak and then decline as lights get brighter (Milner & Do 2017). Sodium channel inactivation from increasing depolarizations accounts for the bright-light decline (Milner & Do 2017). The biophysical properties of M1 ipRGCs determine the setpoint of this depolarization block, and the differences among them distribute intensity encoding across the population (Emanuel et al. 2017). Rod-driven synaptic inputs extend the luminance encoding of M1 ipRGCs to dim light levels. Lee et al. (2019) discovered that a subset of M1 ipRGCs receive no rod input and that the strengths of rod-driven M1 ipRGC responses covary with their dendritic complexity. Thus, morphological, input, and biophysical variation of M1 ipRGCs support robust population encoding of ambient light levels. This gain in luminance resolution comes at the cost of spatial resolution.

4.3.2. Downstream pathways and behavioral significance of retinal luminance signals. M1 ipRGCs send luminance signals to numerous brain areas involved in non-image-forming vision (Hattar et al. 2002, 2006) (**Figure 9*b***). M1 ipRGCs were discovered through their projections to the SCN (Berson et al. 2002). When M1 ipRGCs are ablated, photoentrainment is lost, and circadian rhythms run free (Göz et al. 2008, Güler et al. 2008, Hatori et al. 2008). M1 ipRGCs also provide input to the shell of the olivary pretectal nucleus (OPN) (Hattar et al. 2002, 2006). SCN-projecting and OPN-projecting M1 ipRGCs differ in their expression of the transcription factor Brn3b. SCN-projecting M1 ipRGCs are BRN3b-negative, whereas OPN-projecting M1 ipRGCs are BRN3b-positive (Chen et al. 2011). An intersectional cell ablation strategy revealed that the BRN3b-positive M1 ipRGCs are required for normal pupillary light responses (mediated by the OPN) but dispensable for circadian photoentrainment, which relies on BRN3b-negative M1 ipRGCs (Chen et al. 2011).

M1 ipRGCs exhibit further diversity in their synaptic output. Most M1 ipRGCs release glutamate and the neuropeptide pituitary adenylyl cyclase–activating polypeptide (PCAP) (Engelund et al. 2010, Hannibal et al. 2002). PCAP plays a modulatory role in circadian photoentrainment (Beaulé et al. 2009; Colwell et al. 2004; Kawaguchi et al. 2003, 2010) and supports sustained pupil constriction in response to light (Keenan et al. 2016). Intriguingly, Sonoda et al. (2020) discovered a subset of M1 ipRGCs that releases GABA to dampen the sensitivity of circadian photoentrainment and pupil constriction in response to light. This may explain the discrepancy between the high light sensitivity of M1 ipRGCs and the low light sensitivity of the behaviors they mediate (Sonoda et al. 2020).

Mice are nocturnal rodents that forage at night and sleep in the day. In addition to circadian rhythms in sleep–wake cycles, light pulses early in the night promote sleep acutely (Borbély 1978, Lupi et al. 2008). Different M1 ipRGCs and brain areas mediate the circadian and acute light effects on sleep. BRN3b-negative M1 ipRGC projections to the SCN entrain circadian sleep–wake cycles, whereas BRN3b-positive M1 ipRGC projections to the ventrolateral preoptic nucleus regulate sleep acutely (Rupp et al. 2019).

Projections of BRN3b-negative M1 ipRGCs to the SCN have also been shown to mediate the detrimental effects of shortened (3.5 h–3.5 h) light–dark cycles on spatial learning independent of circadian rhythms, whereas projections of BRN3b-negative M1 ipRGCs to the perihabenular nucleus of the thalamus mediate adverse effects on mood (Fernandez et al. 2018, LeGates et al. 2012). Interestingly, 2–3-h bright-light pulses have been shown to improve spatial learning and increase resilience to adverse stimuli in mice on a normal (12 h–12 h) light–dark cycle. These memory- and mood-enhancing effects of light were shown to be mediated M4 ipRGC (also known as sONα) signals propagating via the IGL and vLGN to the Re and the LHb, respectively (Huang et al. 2019, 2021).

5. REGIONAL SPECIALIZATION AND COLOR PROCESSING

In many species, RGCs are unevenly distributed across the retina. The dendrites of most RGCs maintain constant overlap with same-type neighbors. Therefore, dendritic and receptive field sizes scale as the inverse of RGC density (Masland 2001, Wässle 2004). Areas of high density and small receptive field size are referred to as acute zones (Baden et al. 2020). When looking at the overall RGC density, no acute zones are apparent in the mouse retina (Dräger & Olsen 1981, Jeon et al. 1998). However, Bleckert et al. (2014) discovered that sONα and sOFFα RGCs are packed more densely in the temporal retina, which covers the binocular visual field in mice. Acute zones in the binocular field (i.e., area centralis) are near-universal signs of functional binocular vision (Cartmill 1974, Pettigrew 1986). Therefore, the cell type–specific area centralis suggests that sONα and sOFFα RGCs play an important role in binocular vision of mice.

Additional inhomogeneities in RGC type distributions have been reported for W3 RGCs (enriched in the ventral retina), F RGCs except for F-midi-ON (enriched in the ventral retina), posterior motion–preferring ON-OFF DS RGCs (enriched in the temporal retina), Pix_{ON} RGCs (or M5 ipRGCs, enriched in the nasal retina), and GABAergic M1 ipRGCs (enriched in the dorsotemporal retina) (El-Danaf & Huberman 2019, Rousso et al. 2016, Sonoda et al. 2020, Zhang et al. 2012). In cases where these apparent inhomogeneities were detected by transgenic labeling, independent confirmation is needed. In all cases, the impact of inhomogeneous feature representations on downstream processing and their behavioral purpose remain to be discovered.

Color processing varies along the dorsoventral axis of the mouse retina. Mice have two types of cone photoreceptors: true S-cones, which express only the short-wavelength-sensitive (S-) opsin, and mixed M/S-cones, which coexpress S- and middle-wavelength-sensitive (M-) opsins (Applebury et al. 2000, Haverkamp et al. 2005, Nadal-Nicolás et al. 2020, Ng et al. 2001, Wang et al. 2011). True S-cones are abundant in the ventral retina, where they account for up to 30% of all cones, but are sparse in the dorsal retina (Nadal-Nicolás et al. 2020). Furthermore, mixed M/S-cones express predominantly S-opsin in the ventral and M-opsin in the dorsal retina (Applebury et al. 2000, Haverkamp et al. 2005, Nadal-Nicolás et al. 2020, Ng et al. 2001, Wang et al. 2011). This asymmetry matches the spectral compositions of the upper (sky-dominated) and lower (ground-dominated) visual fields viewed by the ventral and dorsal retina, respectively (Baden et al. 2013).

A dedicated S-cone bipolar cell type (i.e., type 9) has been identified in mice (Breuninger et al. 2011, Haverkamp et al. 2005) and recently shown to be enriched in the ventral retina (Nadal-Nicolás et al. 2020). Blue–yellow opponent RGC types that utilize input from S-cone bipolar cells have been identified in several species (Chichilnisky & Baylor 1999, Dacey & Lee 1994, Sher & DeVries 2012). However, in mice, no single RGC type appears to be dedicated to color-opponent signaling. Instead, color opponency is restricted to the ventral retina and distributed across RGC types (Szatko et al. 2020). In primates, color-opponency relies on circuit comparisons of different cones through type-specific wiring. In mice, the majority of color-opponent RGCs rely on one of two regionally restricted mechanisms. First, in the opsin transition zone around the horizon, RGCs, by chance and position, can have different M- and S-opsin weights in their receptive field center versus surround (Chang et al. 2013). Second, in the ventral retina, some RGCs compare S-opsin-dominant cone input in their center to middle-wavelength-sensitive rod signals in their surround (Joesch & Meister 2016, Szatko et al. 2020). Consistent with these regional mechanisms, color-opponent responses in the dLGN are restricted to the dorsal visual field, and mice can only distinguish chromatic stimuli above the horizon (Denman et al. 2017, 2018).

6. SUMMARY

Recent years have seen tremendous progress in the cataloging of RGCs. Anatomical, functional, and transcriptomic surveys agree that there are more than 40 RGC types in mice (Baden et al. 2016, Bae et al. 2018, Rheaume et al. 2018, Tran et al. 2019). The feature selectivities and circuit mechanisms of only a minority of these cells have been studied in detail, and therefore, much work remains. Beyond filling in these gaps, challenges remain in trying to understand how individual RGCs encode multiple features (i.e., multiplexing), as in sONα RGCs signaling luminance and contrast; how features are encoded in the activity of RGC populations; and how they are extracted from naturalistic stimuli (Turner et al. 2019).

By comparison to our knowledge of RGC types and the circuit mechanisms that underlie their feature preferences, our understanding of the downstream pathways and behavioral significance of RGC signals remains rudimentary. Many of the relevant paragraphs of this review might have ended in "Here be dragons." I hope that more researchers will venture into these scarcely explored territories; trace the projection patterns of more RGC types; and elucidate how their signals are demultiplexed, transformed, and combined with other sensory inputs and information about internal states to guide behavior. This is critical for understanding the retina's diverse contributions to vision and will also anchor investigations of retinal processing.

DISCLOSURE STATEMENT

The author is not aware of any affiliations, memberships, funding, or financial holdings that might be perceived as affecting the objectivity of this review.

ACKNOWLEDGMENTS

The author thanks Dr. Florentina Soto and all members of the Kerschensteiner lab for many helpful discussions and insightful comments on the figures and the manuscript.

LITERATURE CITED

Ahmadlou M, Heimel JA. 2015. Preference for concentric orientations in the mouse superior colliculus. *Nat. Commun.* 6:6773

Antinucci P, Hindges R. 2018. Orientation-selective retinal circuits in vertebrates. *Front. Neural Circuits* 12:11

Applebury ML, Antoch MP, Baxter LC, Chun LL, Falk JD, et al. 2000. The murine cone photoreceptor: a single cone type expresses both S and M opsins with retinal spatial patterning. *Neuron* 27(3):513–23

Aranda ML, Schmidt TM. 2020. Diversity of intrinsically photosensitive retinal ganglion cells: circuits and functions. *Cell. Mol. Life Sci.* 78(3):889–907

Baccus SA, Olveczky BP, Manu M, Meister M. 2008. A retinal circuit that computes object motion. *J. Neurosci.* 28(27):6807–17

Baden T, Berens P, Franke K, Román Rosón M, Bethge M, Euler T. 2016. The functional diversity of retinal ganglion cells in the mouse. *Nature* 529(7586):345–50

Baden T, Euler T, Berens P. 2020. Understanding the retinal basis of vision across species. *Nat. Rev. Neurosci.* 21(1):5–20

Baden T, Schubert T, Chang L, Wei T, Zaichuk M, et al. 2013. A tale of two retinal domains: near-optimal sampling of achromatic contrasts in natural scenes through asymmetric photoreceptor distribution. *Neuron* 80(5):1206–17

Bae JA, Mu S, Kim JS, Turner NL, Tartavull I, et al. 2018. Digital museum of retinal ganglion cells with dense anatomy and physiology. *Cell* 173(5):1293–306.e19

Barlow HB, Hill RM. 1963. Selective sensitivity to direction of movement in ganglion cells of the rabbit retina. *Science* 139(3553):412–14

Barlow HB, Hill RM, Levick WR. 1964. Retinal ganglion cells responding selectively to direction and speed of image motion in the rabbit. *J. Physiol.* 173:377–407

Barlow HB, Levick WR. 1965. The mechanism of directionally selective units in rabbit's retina. *J. Physiol.* 178(3):477–504

Beaulé C, Mitchell JW, Lindberg PT, Damadzic R, Eiden LE, Gillette MU. 2009. Temporally restricted role of retinal PACAP: integration of the phase-advancing light signal to the SCN. *J. Biol. Rhythms* 24(2):126–34

Berson DM, Dunn FA, Takao M. 2002. Phototransduction by retinal ganglion cells that set the circadian clock. *Science* 295(5557):1070–73

Blanchard DC, Williams G, Lee EMC, Blanchard RJ. 1981. Taming of wild *Rattus norvegicus* by lesions of the mesencephalic central gray. *Physiol. Psychol.* 9(2):157–63

Bleckert A, Schwartz GW, Turner MH, Rieke F, Wong ROL. 2014. Visual space is represented by nonmatching topographies of distinct mouse retinal ganglion cell types. *Curr. Biol.* 24(3):310–15

Bloomfield SA. 1994. Orientation-sensitive amacrine and ganglion cells in the rabbit retina. *J. Neurophysiol.* 71(5):1672–91

Borbély AA. 1978. Effects of light on sleep and activity rhythms. *Prog. Neurobiol.* 10(1):1–31

Borghuis BG, Marvin JS, Looger LL, Demb JB. 2013. Two-photon imaging of nonlinear glutamate release dynamics at bipolar cell synapses in the mouse retina. *J. Neurosci.* 33(27):10972–85

Boycott BB, Wässle H. 1974. The morphological types of ganglion cells of the domestic cat's retina. *J. Physiol.* 240(2):397–419

Breuninger T, Puller C, Haverkamp S, Euler T. 2011. Chromatic bipolar cell pathways in the mouse retina. *J. Neurosci.* 31(17):6504–17

Briggman KL, Helmstaedter M, Denk W. 2011. Wiring specificity in the direction-selectivity circuit of the retina. *Nature* 471(7337):183–88

Brüggen B, Meyer A, Boven F, Weiler R, Dedek K. 2015. Type 2 wide-field amacrine cells in TH::GFP mice show a homogenous synapse distribution and contact small ganglion cells. *Eur. J. Neurosci.* 41(6):734–47

Brzezinski JA, Brown NL, Tanikawa A, Bush RA, Sieving PA, et al. 2005. Loss of circadian photoentrainment and abnormal retinal electrophysiology in Math5 mutant mice. *Investig. Ophthalmol. Vis. Sci.* 46(7):2540–51

Cang J, Savier E, Barchini J, Liu X. 2018. Visual function, organization, and development of the mouse superior colliculus. *Annu. Rev. Vis. Sci.* 4:239–62

Cartmill M. 1974. Rethinking primate origins. *Science* 184(4135):436–43

Chandrasekaran AR, Shah RD, Crair MC. 2007. Developmental homeostasis of mouse retinocollicular synapses. *J. Neurosci.* 27(7):1746–55

Chang L, Breuninger T, Euler T. 2013. Chromatic coding from cone-type unselective circuits in the mouse retina. *Neuron* 77(3):559–71

Chen M, Lee S, Park SJH, Looger LL, Zhou ZJ. 2014. Receptive field properties of bipolar cell axon terminals in direction-selective sublaminas of the mouse retina. *J. Neurophysiol.* 112(8):1950–62

Chen M, Lee S, Zhou ZJ. 2017. Local synaptic integration enables ON-OFF asymmetric and layer-specific visual information processing in vGluT3 amacrine cell dendrites. *PNAS* 114(43):11518–23

Chen S-K, Badea TC, Hattar S. 2011. Photoentrainment and pupillary light reflex are mediated by distinct populations of ipRGCs. *Nature* 476(7358):92–95

Chichilnisky EJ, Baylor DA. 1999. Receptive-field microstructure of blue-yellow ganglion cells in primate retina. *Nat. Neurosci.* 2(10):889–93

Colwell CS, Michel S, Itri J, Rodriguez W, Tam J, et al. 2004. Selective deficits in the circadian light response in mice lacking PACAP. *Am. J. Physiol. Regul. Integr. Comp. Physiol.* 287(5):R1194–201

Cooler S, Schwartz GW. 2020. An offset ON-OFF receptive field is created by gap junctions between distinct types of retinal ganglion cells. *Nat. Neurosci.* 24:105–15

Cruz-Martín A, El-Danaf RN, Osakada F, Sriram B, Dhande OS, et al. 2014. A dedicated circuit links direction-selective retinal ganglion cells to the primary visual cortex. *Nature* 507(7492):358–61

Czeisler CA, Shanahan TL, Klerman EB, Martens H, Brotman DJ, et al. 1995. Suppression of melatonin secretion in some blind patients by exposure to bright light. *N. Engl. J. Med.* 332(1):6–11

Dacey DM, Lee BB. 1994. The "blue-on" opponent pathway in primate retina originates from a distinct bistratified ganglion cell type. *Nature* 367(6465):731–35

Dacey DM, Petersen MR. 1992. Dendritic field size and morphology of midget and parasol ganglion cells of the human retina. *PNAS* 89(20):9666–70

De Franceschi G, Vivattanasarn T, Saleem AB, Solomon SG. 2016. Vision guides selection of freeze or flight defense strategies in mice. *Curr. Biol.* 26(16):2150–54

de Malmazet D, Kühn NK, Farrow K. 2018. Retinotopic separation of nasal and temporal motion selectivity in the mouse superior colliculus. *Curr. Biol.* 28(18):2961–69.e4

de Monasterio FM. 1978. Properties of ganglion cells with atypical receptive-field organization in retina of macaques. *J. Neurophysiol.* 41(6):1435–49

Dean P, Redgrave P, Westby GW. 1989. Event or emergency? Two response systems in the mammalian superior colliculus. *Trends Neurosci.* 12(4):137–47

Della Santina L, Kuo SP, Yoshimatsu T, Okawa H, Suzuki SC, et al. 2016. Glutamatergic monopolar interneurons provide a novel pathway of excitation in the mouse retina. *Curr. Biol.* 26(15):2070–77

Delorme A, Richard G, Fabre-Thorpe M. 2000. Ultra-rapid categorisation of natural scenes does not rely on colour cues: a study in monkeys and humans. *Vis. Res.* 40(16):2187–200

Demb JB, Singer JH. 2015. Functional circuitry of the retina. *Annu. Rev. Vis. Sci.* 1:263–89

Denman DJ, Luviano JA, Ollerenshaw DR, Cross S, Williams D, et al. 2018. Mouse color and wavelength-specific luminance contrast sensitivity are non-uniform across visual space. *eLife* 7:e31209

Denman DJ, Siegle JH, Koch C, Reid RC, Blanche TJ. 2017. Spatial organization of chromatic pathways in the mouse dorsal lateral geniculate nucleus. *J. Neurosci.* 37(5):1102–16

Dhande OS, Estevez ME, Quattrochi LE, El-Danaf RN, Nguyen PL, et al. 2013. Genetic dissection of retinal inputs to brainstem nuclei controlling image stabilization. *J. Neurosci.* 33(45):17797–813

Diamond JS. 2017. Inhibitory interneurons in the retina: types, circuitry, and function. *Annu. Rev. Vis. Sci.* 3:1–24

Ding H, Smith RG, Poleg-Polsky A, Diamond JS, Briggman KL. 2016. Species-specific wiring for direction selectivity in the mammalian retina. *Nature* 535(7610):105–10

Do MTH. 2019. Melanopsin and the intrinsically photosensitive retinal ganglion cells: biophysics to behavior. *Neuron* 104(2):205–26

Do MTH, Yau K-W. 2010. Intrinsically photosensitive retinal ganglion cells. *Physiol. Rev.* 90(4):1547–81

Dräger UC, Olsen JF. 1981. Ganglion cell distribution in the retina of the mouse. *Investig. Ophthalmol. Vis. Sci.* 20(3):285–93

Dumitrescu ON, Pucci FG, Wong KY, Berson DM. 2009. Ectopic retinal ON bipolar cell synapses in the OFF inner plexiform layer: contacts with dopaminergic amacrine cells and melanopsin ganglion cells. *J. Comp. Neurol.* 517(2):226–44

Ebihara S, Tsuji K. 1980. Entrainment of the circadian activity rhythm to the light cycle: effective light intensity for a Zeitgeber in the retinal degenerate C3H mouse and the normal C57BL mouse. *Physiol. Behav.* 24(3):523–27

Ecker JL, Dumitrescu ON, Wong KY, Alam NM, Chen S-K, et al. 2010. Melanopsin-expressing retinal ganglion-cell photoreceptors: cellular diversity and role in pattern vision. *Neuron* 67(1):49–60

El-Danaf RN, Huberman AD. 2019. Sub-topographic maps for regionally enhanced analysis of visual space in the mouse retina. *J. Comp. Neurol.* 527(1):259–69

Ellis EM, Gauvain G, Sivyer B, Murphy GJ. 2016. Shared and distinct retinal input to the mouse superior colliculus and dorsal lateral geniculate nucleus. *J. Neurophysiol.* 116(2):602–10

Elstrott J, Anishchenko A, Greschner M, Sher A, Litke AM, et al. 2008. Direction selectivity in the retina is established independent of visual experience and cholinergic retinal waves. *Neuron* 58(4):499–506

Emanuel AJ, Kapur K, Do MTH. 2017. Biophysical variation within the M1 type of ganglion cell photoreceptor. *Cell Rep.* 21(4):1048–62

Engelund A, Fahrenkrug J, Harrison A, Hannibal J. 2010. Vesicular glutamate transporter 2 (VGLUT2) is co-stored with PACAP in projections from the rat melanopsin-containing retinal ganglion cells. *Cell Tissue Res.* 340(2):243–55

Euler T, Detwiler PB, Denk W. 2002. Directionally selective calcium signals in dendrites of starburst amacrine cells. *Nature* 418(6900):845–52

Euler T, Haverkamp S, Schubert T, Baden T. 2014. Retinal bipolar cells: elementary building blocks of vision. *Nat. Rev. Neurosci.* 15(8):507–19

Evans DA, Stempel AV, Vale R, Branco T. 2019. Cognitive control of escape behaviour. *Trends Cogn. Sci.* 23(4):334–48

Evans DA, Stempel AV, Vale R, Ruehle S, Lefler Y, Branco T. 2018. A synaptic threshold mechanism for computing escape decisions. *Nature* 558(7711):590–94

Famiglietti EV. 1991. Synaptic organization of starburst amacrine cells in rabbit retina: analysis of serial thin sections by electron microscopy and graphic reconstruction. *J. Comp. Neurol.* 309(1):40–70

Faulstich BM, Onori KA, du Lac S. 2004. Comparison of plasticity and development of mouse optokinetic and vestibulo-ocular reflexes suggests differential gain control mechanisms. *Vis. Res.* 44(28):3419–27

Feinberg EH, Meister M. 2015. Orientation columns in the mouse superior colliculus. *Nature* 519(7542):229–32

Fernandez DC, Fogerson PM, Lazzerini Ospri L, Thomsen MB, Layne RM, et al. 2018. Light affects mood and learning through distinct retina-brain pathways. *Cell* 175(1):71–84.e18

Fiscella M, Franke F, Farrow K, Müller J, Roska B, et al. 2015. Visual coding with a population of direction-selective neurons. *J. Neurophysiol.* 114(4):2485–99

Fotowat H, Gabbiani F. 2011. Collision detection as a model for sensory-motor integration. *Annu. Rev. Neurosci.* 34:1–19

Franke K, Berens P, Schubert T, Bethge M, Euler T, Baden T. 2017. Inhibition decorrelates visual feature representations in the inner retina. *Nature* 542(7642):439–44

Fransen JW, Borghuis BG. 2017. Temporally diverse excitation generates direction-selective responses in ON- and OFF-type retinal starburst amacrine cells. *Cell Rep.* 18(6):1356–65

Freedman MS, Lucas RJ, Soni B, von Schantz M, Muñoz M, et al. 1999. Regulation of mammalian circadian behavior by non-rod, non-cone, ocular photoreceptors. *Science* 284(5413):502–4

Fried SI, Münch TA, Werblin FS. 2002. Mechanisms and circuitry underlying directional selectivity in the retina. *Nature* 420(6914):411–14

Frost BJ. 2010. A taxonomy of different forms of visual motion detection and their underlying neural mechanisms. *Brain Behav. Evol.* 75(3):218–35

Gale SD, Murphy GJ. 2014. Distinct representation and distribution of visual information by specific cell types in mouse superficial superior colliculus. *J. Neurosci.* 34(40):13458–71

Gale SD, Murphy GJ. 2016. Active dendritic properties and local inhibitory input enable selectivity for object motion in mouse superior colliculus neurons. *J. Neurosci.* 36(35):9111–23

Gauvain G, Murphy GJ. 2015. Projection-specific characteristics of retinal input to the brain. *J. Neurosci.* 35(16):6575–83

Göz D, Studholme K, Lappi DA, Rollag MD, Provencio I, Morin LP. 2008. Targeted destruction of photosensitive retinal ganglion cells with a saporin conjugate alters the effects of light on mouse circadian rhythms. *PLOS ONE* 3(9):e3153

Greene MJ, Kim JS, Seung HS, EyeWirers. 2016. Analogous convergence of sustained and transient inputs in parallel On and Off pathways for retinal motion computation. *Cell Rep*. 14(8):1892–900

Grimes WN, Schwartz GW, Rieke F. 2014. The synaptic and circuit mechanisms underlying a change in spatial encoding in the retina. *Neuron* 82(2):460–73

Grubb MS, Thompson ID. 2003. Quantitative characterization of visual response properties in the mouse dorsal lateral geniculate nucleus. *J. Neurophysiol.* 90(6):3594–607

Güler AD, Ecker JL, Lall GS, Haq S, Altimus CM, et al. 2008. Melanopsin cells are the principal conduits for rod-cone input to non-image-forming vision. *Nature* 453(7191):102–5

Hammer S, Monavarfeshani A, Lemon T, Su J, Fox MA. 2015. Multiple retinal axons converge onto relay cells in the adult mouse thalamus. *Cell Rep*. 12(10):1575–83

Hannibal J, Hindersson P, Knudsen SM, Georg B, Fahrenkrug J. 2002. The photopigment melanopsin is exclusively present in pituitary adenylate cyclase-activating polypeptide-containing retinal ganglion cells of the retinohypothalamic tract. *J. Neurosci.* 22(1):RC191

Hatori M, Le H, Vollmers C, Keding SR, Tanaka N, et al. 2008. Inducible ablation of melanopsin-expressing retinal ganglion cells reveals their central role in non-image forming visual responses. *PLOS ONE* 3(6):e2451

Hattar S, Kumar M, Park A, Tong P, Tung J, et al. 2006. Central projections of melanopsin-expressing retinal ganglion cells in the mouse. *J. Comp. Neurol.* 497(3):326–49

Hattar S, Liao HW, Takao M, Berson DM, Yau KW. 2002. Melanopsin-containing retinal ganglion cells: architecture, projections, and intrinsic photosensitivity. *Science* 295(5557):1065–70

Hausselt SE, Euler T, Detwiler PB, Denk W. 2007. A dendrite-autonomous mechanism for direction selectivity in retinal starburst amacrine cells. *PLOS Biol.* 5(7):e185

Haverkamp S, Wässle H, Duebel J, Kuner T, Augustine GJ, et al. 2005. The primordial, blue-cone color system of the mouse retina. *J. Neurosci.* 25(22):5438–45

Helmstaedter M, Briggman KL, Turaga SC, Jain V, Seung HS, Denk W. 2013. Connectomic reconstruction of the inner plexiform layer in the mouse retina. *Nature* 500(7461):168–74

Hillier D, Fiscella M, Drinnenberg A, Trenholm S, Rompani SB, et al. 2017. Causal evidence for retina-dependent and -independent visual motion computations in mouse cortex. *Nat. Neurosci.* 20:960–68

Hofbauer A, Dräger UC. 1985. Depth segregation of retinal ganglion cells projecting to mouse superior colliculus. *J. Comp. Neurol.* 234(4):465–74

Hoggarth A, McLaughlin AJ, Ronellenfitch K, Trenholm S, Vasandani R, et al. 2015. Specific wiring of distinct amacrine cells in the directionally selective retinal circuit permits independent coding of direction and size. *Neuron* 86(1):276–91

Hong YK, Burr EF, Sanes JR, Chen C. 2018. Heterogeneity of retinogeniculate axon arbors. *Eur. J. Neurosci.* 49(7):948–56

Hong YK, Kim I-J, Sanes JR. 2011. Stereotyped axonal arbors of retinal ganglion cell subsets in the mouse superior colliculus. *J. Comp. Neurol.* 519(9):1691–711

Hoshi H, Liu W-L, Massey SC, Mills SL. 2009. ON inputs to the OFF layer: bipolar cells that break the stratification rules of the retina. *J. Neurosci.* 29(28):8875–83

Hoy JL, Bishop HI, Niell CM. 2019. Defined cell types in superior colliculus make distinct contributions to prey capture behavior in the mouse. *Curr. Biol.* 29(23):4130–38.e5

Hsiang J-C, Johnson KP, Madisen L, Zeng H, Kerschensteiner D. 2017. Local processing in neurites of VGluT3-expressing amacrine cells differentially organizes visual information. *eLife* 6:e31307

Huang L, Xi Y, Peng Y, Yang Y, Huang X, et al. 2019. A visual circuit related to habenula underlies the antidepressive effects of light therapy. *Neuron* 102(1):128–42.e8

Huang L, Yuan T, Tan M, Xi Y, Hu Y, et al. 2017. A retinoraphe projection regulates serotonergic activity and looming-evoked defensive behaviour. *Nat. Commun.* 8:14908

Huang X, Huang P, Huang L, Hu Z, Liu X, et al. 2021. A visual circuit related to the nucleus reuniens for the spatial-memory-promoting effects of light treatment. *Neuron* 109(2):347–62.e7

Hubel DH, Wiesel TN. 1962. Receptive fields, binocular interaction and functional architecture in the cat's visual cortex. *J. Physiol.* 160:106–54

Huberman AD, Manu M, Koch SM, Susman MW, Lutz AB, et al. 2008. Architecture and activity-mediated refinement of axonal projections from a mosaic of genetically identified retinal ganglion cells. *Neuron* 59(3):425–38

Huberman AD, Wei W, Elstrott J, Stafford BK, Feller MB, Barres BA. 2009. Genetic identification of an On-Off direction-selective retinal ganglion cell subtype reveals a layer-specific subcortical map of posterior motion. *Neuron* 62(3):327–34

Inayat S, Barchini J, Chen H, Feng L, Liu X, Cang J. 2015. Neurons in the most superficial lamina of the mouse superior colliculus are highly selective for stimulus direction. *J. Neurosci.* 35(20):7992–8003

Ito S, Feldheim DA. 2018. The mouse superior colliculus: an emerging model for studying circuit formation and function. *Front. Neural Circuits* 12:10

Ito S, Feldheim DA, Litke AM. 2017. Segregation of visual response properties in the mouse superior colliculus and their modulation during locomotion. *J. Neurosci.* 37(35):8428–43

Ivanova E, Lee P, Pan Z-H. 2013. Characterization of multiple bistratified retinal ganglion cells in a Purkinje cell protein 2-Cre transgenic mouse line. *J. Comp. Neurol.* 521(9):2165–80

Jacoby J, Schwartz GW. 2017. Three small-receptive-field ganglion cells in the mouse retina are distinctly tuned to size, speed, and object motion. *J. Neurosci.* 37(3):610–25

Jacoby J, Schwartz GW. 2018. Typology and circuitry of suppressed-by-contrast retinal ganglion cells. *Front. Cell. Neurosci.* 12:269

Jacoby J, Zhu Y, DeVries SH, Schwartz GW. 2015. An amacrine cell circuit for signaling steady illumination in the retina. *Cell Rep.* 13(12):2663–70

Jeon CJ, Strettoi E, Masland RH. 1998. The major cell populations of the mouse retina. *J. Neurosci.* 18(21):8936–46

Jiang Z, Yue WWS, Chen L, Sheng Y, Yau K-W. 2018. Cyclic-nucleotide- and HCN-channel-mediated phototransduction in intrinsically photosensitive retinal ganglion cells. *Cell* 175(3):652–64.e12

Joesch M, Meister M. 2016. A neuronal circuit for colour vision based on rod-cone opponency. *Nature* 532(7598):236–39

Johnson KP, Zhao L, Kerschensteiner D. 2018. A pixel-encoder retinal ganglion cell with spatially offset excitatory and inhibitory receptive fields. *Cell Rep.* 22(6):1462–72

Johnston J, Seibel S-H, Darnet LSA, Renninger S, Orger M, Lagnado L. 2019. A retinal circuit generating a dynamic predictive code for oriented features. *Neuron* 102(6):1211–22.e3

Kaplan E. 2008. Luminance sensitivity and contrast detection. In *The Senses: A Comprehensive Reference*, Vol. 2, ed. RH Masland, TD Albright, P Dallos, D Oertel, S Firestein, et al., pp. 29–43. Amsterdam: Elsevier

Kawaguchi C, Isojima Y, Shintani N, Hatanaka M, Guo X, et al. 2010. PACAP-deficient mice exhibit light parameter-dependent abnormalities on nonvisual photoreception and early activity onset. *PLOS ONE* 5(2):e9286

Kawaguchi C, Tanaka K, Isojima Y, Shintani N, Hashimoto H, et al. 2003. Changes in light-induced phase shift of circadian rhythm in mice lacking PACAP. *Biochem. Biophys. Res. Commun.* 310(1):169–75

Kay JN, De la Huerta I, Kim I-J, Zhang Y, Yamagata M, et al. 2011. Retinal ganglion cells with distinct directional preferences differ in molecular identity, structure, and central projections. *J. Neurosci.* 31(21):7753–62

Keenan WT, Rupp AC, Ross RA, Somasundaram P, Hiriyanna S, et al. 2016. A visual circuit uses complementary mechanisms to support transient and sustained pupil constriction. *eLife* 5:e15392

Kerschensteiner D, Guido W. 2017. Organization of the dorsal lateral geniculate nucleus in the mouse. *Vis. Neurosci.* 34:E008

Kim I-J, Zhang Y, Meister M, Sanes JR. 2010. Laminar restriction of retinal ganglion cell dendrites and axons: subtype-specific developmental patterns revealed with transgenic markers. *J. Neurosci.* 30(4):1452–62

Kim I-J, Zhang Y, Yamagata M, Meister M, Sanes JR. 2008. Molecular identification of a retinal cell type that responds to upward motion. *Nature* 452(7186):478–82

Kim JS, Greene MJ, Zlateski A, Lee K, Richardson M, et al. 2014. Space-time wiring specificity supports direction selectivity in the retina. *Nature* 509(7500):331–36

Kim T, Kerschensteiner D. 2017. Inhibitory control of feature selectivity in an object motion sensitive circuit of the retina. *Cell Rep*. 19(7):1343–50

Kim T, Shen N, Hsiang J-C, Johnson KP, Kerschensteiner D. 2020. Dendritic and parallel processing of visual threats in the retina control defensive responses. *Sci. Adv.* 6(47):eabc9920

Kim T, Soto F, Kerschensteiner D. 2015. An excitatory amacrine cell detects object motion and provides feature-selective input to ganglion cells in the mouse retina. *eLife* 4:e08025

Kingdom FAA, Prins N. 2016. *Psychophysics: A Practical Introduction*. Cambridge, MA: Academic

Knop GC, Feigenspan A, Weiler R, Dedek K. 2011. Inputs underlying the ON-OFF light responses of type 2 wide-field amacrine cells in TH::GFP mice. *J. Neurosci.* 31(13):4780–91

Koren D, Grove JCR, Wei W. 2017. Cross-compartmental modulation of dendritic signals for retinal direction selectivity. *Neuron* 95(4):914–27.e4

Krauzlis RJ, Lovejoy LP, Zénon A. 2013. Superior colliculus and visual spatial attention. *Annu. Rev. Neurosci.* 36:165–82

Krieger B, Qiao M, Rousso DL, Sanes JR, Meister M. 2017. Four alpha ganglion cell types in mouse retina: function, structure, and molecular signatures. *PLOS ONE* 12(7):e0180091

Krishnaswamy A, Yamagata M, Duan X, Hong YK, Sanes JR. 2015. Sidekick 2 directs formation of a retinal circuit that detects differential motion. *Nature* 524(7566):466–70

Kuffler SW. 1953. Discharge patterns and functional organization of mammalian retina. *J. Neurophysiol.* 16(1):37–68

Kuo SP, Schwartz GW, Rieke F. 2016. Nonlinear spatiotemporal integration by electrical and chemical synapses in the retina. *Neuron* 90(2):320–32

Lazzerini Ospri L, Prusky G, Hattar S. 2017. Mood, the circadian system, and melanopsin retinal ganglion cells. *Annu. Rev. Neurosci.* 40:539–56

Lee KH, Tran A, Turan Z, Meister M. 2020. The sifting of visual information in the superior colliculus. *eLife* 9:e50678

Lee S, Chen L, Chen M, Ye M, Seal RP, Zhou ZJ. 2014. An unconventional glutamatergic circuit in the retina formed by vGluT3 amacrine cells. *Neuron* 84(4):708–15

Lee S, Kim K, Zhou ZJ. 2010. Role of ACh-GABA cotransmission in detecting image motion and motion direction. *Neuron* 68(6):1159–72

Lee S, Zhang Y, Chen M, Zhou ZJ. 2016. Segregated glycine-glutamate co-transmission from vGluT3 amacrine cells to contrast-suppressed and contrast-enhanced retinal circuits. *Neuron* 90(1):27–34

Lee S, Zhou ZJ. 2006. The synaptic mechanism of direction selectivity in distal processes of starburst amacrine cells. *Neuron* 51(6):787–99

Lee SK, Sonoda T, Schmidt TM. 2019. M1 intrinsically photosensitive retinal ganglion cells integrate rod and melanopsin inputs to signal in low light. *Cell Rep*. 29(11):3349–55.e2

LeGates TA, Altimus CM, Wang H, Lee H-K, Yang S, et al. 2012. Aberrant light directly impairs mood and learning through melanopsin-expressing neurons. *Nature* 491(7425):594–98

Levick WR. 1967. Receptive fields and trigger features of ganglion cells in the visual streak of the rabbits retina. *J. Physiol.* 188(3):285–307

Levine JN, Schwartz GW. 2020. The olivary pretectal nucleus receives visual input of high spatial resolution. bioRxiv 2020.06.23.168054. **https://doi.org/10.1101/2020.06.23.168054**

Liang F, Xiong XR, Zingg B, Ji X-Y, Zhang LI, Tao HW. 2015. Sensory cortical control of a visually induced arrest behavior via corticotectal projections. *Neuron* 86(3):755–67

Liang L, Chen C. 2020. Organization, function, and development of the mouse retinogeniculate synapse. *Annu. Rev. Vis. Sci.* 6:261–85

Liang L, Fratzl A, Goldey G, Ramesh RN, Sugden AU, et al. 2018. A fine-scale functional logic to convergence from retina to thalamus. *Cell* 173(6):1343–55.e24

Lien AD, Scanziani M. 2013. Tuned thalamic excitation is amplified by visual cortical circuits. *Nat. Neurosci.* 16(9):1315–23

Lien AD, Scanziani M. 2018. Cortical direction selectivity emerges at convergence of thalamic synapses. *Nature* 558(7708):80–86

Lilley BN, Sabbah S, Hunyara JL, Gribble KD, Al-Khindi T, et al. 2019. Genetic access to neurons in the accessory optic system reveals a role for Sema6A in midbrain circuitry mediating motion perception. *J. Comp. Neurol.* 527(1):282–96

Litvina EY, Chen C. 2017. Functional convergence at the retinogeniculate synapse. *Neuron* 96(2):330–38.e5

Liu B-H, Li P, Sun YJ, Li Y-T, Zhang LI, Tao HW. 2010. Intervening inhibition underlies simple-cell receptive field structure in visual cortex. *Nat. Neurosci.* 13(1):89–96

Lucas RJ, Freedman MS, Muñoz M, Garcia-Fernández JM, Foster RG. 1999. Regulation of the mammalian pineal by non-rod, non-cone, ocular photoreceptors. *Science* 284(5413):505–7

Lupi D, Oster H, Thompson S, Foster RG. 2008. The acute light-induction of sleep is mediated by OPN4-based photoreception. *Nat. Neurosci.* 11(9):1068–73

Mani A, Schwartz GW. 2017. Circuit mechanisms of a retinal ganglion cell with stimulus-dependent response latency and activation beyond its dendrites. *Curr. Biol.* 27(4):471–82

Margolis DJ, Detwiler PB. 2007. Different mechanisms generate maintained activity in ON and OFF retinal ganglion cells. *J. Neurosci.* 27(22):5994–6005

Marshel JH, Kaye AP, Nauhaus I, Callaway EM. 2012. Anterior-posterior direction opponency in the superficial mouse lateral geniculate nucleus. *Neuron* 76(4):713–20

Martersteck EM, Hirokawa KE, Evarts M, Bernard A, Duan X, et al. 2017. Diverse central projection patterns of retinal ganglion cells. *Cell Rep.* 18(8):2058–72

Masland RH. 2001. The fundamental plan of the retina. *Nat. Neurosci.* 4(9):877–86

Masland RH, Martin PR. 2007. The unsolved mystery of vision. *Curr. Biol.* 17(15):R577–82

Matsumoto A, Agbariah W, Nolte SS, Andrawos R, Levi H, et al. 2020. Synapse-specific direction selectivity in retinal bipolar cell axon terminals. bioRxiv 2020.10.12.335810. **https://doi.org/10.1101/2020.10.12.335810**

Matsumoto A, Briggman KL, Yonehara K. 2019. Spatiotemporally asymmetric excitation supports mammalian retinal motion sensitivity. *Curr. Biol.* 29(19):3277–88.e5

Maturana HR, Frenk S. 1963. Directional movement and horizontal edge detectors in the pigeon retina. *Science* 142(3594):977–79

Mauss AS, Vlasits A, Borst A, Feller M. 2017. Visual circuits for direction selectivity. *Annu. Rev. Neurosci.* 40:211–30

Meyer AF, O'Keefe J, Poort J. 2020. Two distinct types of eye-head coupling in freely moving mice. *Curr. Biol.* 30(11):2116–30.e6

Meyer AF, Poort J, O'Keefe J, Sahani M, Linden JF. 2018. A head-mounted camera system integrates detailed behavioral monitoring with multichannel electrophysiology in freely moving mice. *Neuron* 100(1):46–60.e7

Michaiel AM, Abe ETT, Niell CM. 2020. Dynamics of gaze control during prey capture in freely moving mice. *eLife* 9:e57458

Milner ES, Do MTH. 2017. A population representation of absolute light intensity in the mammalian retina. *Cell* 171(4):865–76.e16

Monavarfeshani A, Sabbagh U, Fox MA. 2017. Not a one-trick pony: diverse connectivity and functions of the rodent lateral geniculate complex. *Vis. Neurosci.* 34:E012

Morgan JL, Berger DR, Wetzel AW, Lichtman JW. 2016. The fuzzy logic of network connectivity in mouse visual thalamus. *Cell* 165(1):192–206

Morgan JL, Soto F, Wong ROL, Kerschensteiner D. 2011. Development of cell type-specific connectivity patterns of converging excitatory axons in the retina. *Neuron* 71(6):1014–21

Morin LP, Studholme KM. 2014. Retinofugal projections in the mouse. *J. Comp. Neurol.* 522(16):3733–53

Morrie RD, Feller MB. 2018. A dense starburst plexus is critical for generating direction selectivity. *Curr. Biol.* 28(8):1204–12.e5

Münch TA, da Silveira RA, Siegert S, Viney TJ, Awatramani GB, Roska B. 2009. Approach sensitivity in the retina processed by a multifunctional neural circuit. *Nat. Neurosci.* 12(10):1308–16

Murphy GJ, Rieke F. 2006. Network variability limits stimulus-evoked spike timing precision in retinal ganglion cells. *Neuron* 52(3):511–24

Murphy GJ, Rieke F. 2011. Electrical synaptic input to ganglion cells underlies differences in the output and absolute sensitivity of parallel retinal circuits. *J. Neurosci.* 31(34):12218–28

Murphy-Baum BL, Taylor WR. 2015. The synaptic and morphological basis of orientation selectivity in a polyaxonal amacrine cell of the rabbit retina. *J. Neurosci.* 35(39):13336–50

Nadal-Nicolás FM, Kunze VP, Ball JM, Peng BT, Krishnan A, et al. 2020. True S-cones are concentrated in the ventral mouse retina and wired for color detection in the upper visual field. *eLife* 9:e56840

Nath A, Schwartz GW. 2016. Cardinal orientation selectivity is represented by two distinct ganglion cell types in mouse retina. *J. Neurosci.* 36(11):3208–21

Nath A, Schwartz GW. 2017. Electrical synapses convey orientation selectivity in the mouse retina. *Nat. Commun.* 8:2025

Ng L, Hurley JB, Dierks B, Srinivas M, Saltó C, et al. 2001. A thyroid hormone receptor that is required for the development of green cone photoreceptors. *Nat. Genet.* 27(1):94–98

Niell CM. 2013. Vision: more than expected in the early visual system. *Curr. Biol.* 23(16):R681–84

Niell CM, Stryker MP. 2010. Modulation of visual responses by behavioral state in mouse visual cortex. *Neuron* 65(4):472–79

Olveczky BP, Baccus SA, Meister M. 2003. Segregation of object and background motion in the retina. *Nature* 423(6938):401–8

Osterhout JA, Stafford BK, Nguyen PL, Yoshihara Y, Huberman AD. 2015. Contactin-4 mediates axon-target specificity and functional development of the accessory optic system. *Neuron* 86(4):985–99

Pang J-J, Gao F, Wu SM. 2003. Light-evoked excitatory and inhibitory synaptic inputs to ON and OFF α ganglion cells in the mouse retina. *J. Neurosci.* 23(14):6063–73

Park SJH, Kim I-J, Looger LL, Demb JB, Borghuis BG. 2014. Excitatory synaptic inputs to mouse on-off direction-selective retinal ganglion cells lack direction tuning. *J. Neurosci.* 34(11):3976–81

Park SJH, Pottackal J, Ke J-B, Jun NY, Rahmani P, et al. 2018. Convergence and divergence of CRH amacrine cells in mouse retinal circuitry. *J. Neurosci.* 38(15):3753–66

Pearson JT, Kerschensteiner D. 2015. Ambient illumination switches contrast preference of specific retinal processing streams. *J. Neurophysiol.* 114(1):540–50

Peek MY, Card GM. 2016. Comparative approaches to escape. *Curr. Opin. Neurobiol.* 41:167–73

Pei Z, Chen Q, Koren D, Giammarinaro B, Acaron Ledesma H, Wei W. 2015. Conditional knock-out of vesicular GABA transporter gene from starburst amacrine cells reveals the contributions of multiple synaptic mechanisms underlying direction selectivity in the retina. *J. Neurosci.* 35(38):13219–32

Peichl L, Buhl EH, Boycott BB. 1987. Alpha ganglion cells in the rabbit retina. *J. Comp. Neurol.* 263(1):25–41

Pettigrew JD. 1986. Evolution of binocular vision. In *Visual Neuroscience*, ed. JD Pettigrew, KJ Sanderson, WR Levick, pp. 208–22. Cambridge, UK: Cambridge Univ. Press

Piscopo DM, El-Danaf RN, Huberman AD, Niell CM. 2013. Diverse visual features encoded in mouse lateral geniculate nucleus. *J. Neurosci.* 33(11):4642–56

Poleg-Polsky A, Ding H, Diamond JS. 2018. Functional compartmentalization within starburst amacrine cell dendrites in the retina. *Cell Rep.* 22(11):2898–908

Provencio I, Jiang G, De Grip WJ, Hayes WP, Rollag MD. 1998. Melanopsin: an opsin in melanophores, brain, and eye. *PNAS* 95(1):340–45

Provencio I, Rodriguez IR, Jiang G, Hayes WP, Moreira EF, Rollag MD. 2000. A novel human opsin in the inner retina. *J. Neurosci.* 20(2):600–5

Quattrochi LE, Stabio ME, Kim I, Ilardi MC, Fogerson PM, et al. 2018. The M6 cell: a small-field bistratified photosensitive retinal ganglion cell. *J. Comp. Neurol.* 527(1):297–311

Rasmussen R, Matsumoto A, Dahlstrup Sietam M, Yonehara K. 2020. A segregated cortical stream for retinal direction selectivity. *Nat. Commun.* 11:831

Rasmussen R, Yonehara K. 2020. Contributions of retinal direction selectivity to central visual processing. *Curr. Biol.* 30(15):R897–903

Reinhard K, Kühn NK, Farrow K. 2020. Direction selectivity in the retina and beyond. In *The Senses: A Comprehensive Reference*, ed. B Fritzsch, pp. 423–46. Amsterdam: Elsevier. 2nd ed.

Reinhard K, Li C, Do Q, Burke EG, Heynderickx S, Farrow K. 2019. A projection specific logic to sampling visual inputs in mouse superior colliculus. *eLife* 8:e50697

Rheaume BA, Jereen A, Bolisetty M, Sajid MS, Yang Y, et al. 2018. Single cell transcriptome profiling of retinal ganglion cells identifies cellular subtypes. *Nat. Commun.* 9:2759

Rieke F, Rudd ME. 2009. The challenges natural images pose for visual adaptation. *Neuron* 64(5):605–16
Rivlin-Etzion M, Zhou K, Wei W, Elstrott J, Nguyen PL, et al. 2011. Transgenic mice reveal unexpected diversity of on-off direction-selective retinal ganglion cell subtypes and brain structures involved in motion processing. *J. Neurosci.* 31(24):8760–69
Rodieck RW. 1967. Receptive fields in the cat retina: a new type. *Science* 157(3784):90–92
Román Rosón M, Bauer Y, Kotkat AH, Berens P, Euler T, Busse L. 2019. Mouse dLGN receives functional input from a diverse population of retinal ganglion cells with limited convergence. *Neuron* 102(2):462–76.e8
Rompani SB, Müllner FE, Wanner A, Zhang C, Roth CN, et al. 2017. Different modes of visual integration in the lateral geniculate nucleus revealed by single-cell-initiated transsynaptic tracing. *Neuron* 93(4):767–76.e6
Rousso DL, Qiao M, Kagan RD, Yamagata M, Palmiter RD, Sanes JR. 2016. Two pairs of ON and OFF retinal ganglion cells are defined by intersectional patterns of transcription factor expression. *Cell Rep.* 15(9):1930–44
Rupp AC, Ren M, Altimus CM, Fernandez DC, Richardson M, et al. 2019. Distinct ipRGC subpopulations mediate light's acute and circadian effects on body temperature and sleep. *eLife* 8:e44358
Sabbah S, Gemmer JA, Bhatia-Lin A, Manoff G, Castro G, et al. 2017. A retinal code for motion along the gravitational and body axes. *Nature* 546(7659):492–97
Sabbah S, Papendorp C, Koplas E, Beltoja M. 2018. Synaptic circuits for irradiance coding by intrinsically photosensitive retinal ganglion cells. bioRxiv 442954. **https://doi.org/10.1101/442954**
Sahibzada N, Dean P, Redgrave P. 1986. Movements resembling orientation or avoidance elicited by electrical stimulation of the superior colliculus in rats. *J. Neurosci.* 6(3):723–33
Sanes JR, Zipursky SL. 2010. Design principles of insect and vertebrate visual systems. *Neuron* 66(1):15–36
Schmidt TM, Alam NM, Chen S, Kofuji P, Li W, et al. 2014. A role for melanopsin in alpha retinal ganglion cells and contrast detection. *Neuron* 82(4):781–88
Scholl B, Tan AYY, Corey J, Priebe NJ. 2013. Emergence of orientation selectivity in the mammalian visual pathway. *J. Neurosci.* 33(26):10616–24
Schwartz GW, Okawa H, Dunn FA, Morgan JL, Kerschensteiner D, et al. 2012. The spatial structure of a nonlinear receptive field. *Nat. Neurosci.* 15(11):1572–80
Schwartz GW, Swygart D. 2020. Circuits for feature selectivity in the inner retina. In *The Senses: A Comprehensive Reference*, ed. B Fritzsch, pp. 275–92. Amsterdam: Elsevier. 2nd ed.
Sethuramanujam S, McLaughlin AJ, deRosenroll G, Hoggarth A, Schwab DJ, Awatramani GB. 2016. A central role for mixed acetylcholine/GABA transmission in direction coding in the retina. *Neuron* 90(6):1243–56
Shang C, Chen Z, Liu A, Li Y, Zhang J, et al. 2018. Divergent midbrain circuits orchestrate escape and freezing responses to looming stimuli in mice. *Nat. Commun.* 9:1232
Shang C, Liu Z, Chen Z, Shi Y, Wang Q, et al. 2015. A parvalbumin-positive excitatory visual pathway to trigger fear responses in mice. *Science* 348(6242):1472–77
Shekhar K, Lapan SW, Whitney IE, Tran NM, Macosko EZ, et al. 2016. Comprehensive classification of retinal bipolar neurons by single-cell transcriptomics. *Cell* 166(5):1308–23.e30
Shen N, Wang B, Soto F, Kerschensteiner D. 2020. Homeostatic plasticity shapes the retinal response to photoreceptor degeneration. *Curr. Biol.* 30(10):1916–26.e3
Sher A, DeVries SH. 2012. A non-canonical pathway for mammalian blue-green color vision. *Nat. Neurosci.* 15(7):952–53
Shi X, Barchini J, Ledesma HA, Koren D, Jin Y, et al. 2017. Retinal origin of direction selectivity in the superior colliculus. *Nat. Neurosci.* 20(4):550–58
Sillar KT, Picton LD, Heitler WJ. 2016. *The Neuroethology of Predation and Escape*. Hoboken, NJ: Wiley
Simpson JI. 1984. The accessory optic system. *Annu. Rev. Neurosci.* 7:13–41
Sinha R, Hoon M, Baudin J, Okawa H, Wong ROL, Rieke F. 2017. Cellular and circuit mechanisms shaping the perceptual properties of the primate fovea. *Cell* 168(3):413–26.e12
Sivyer B, Taylor WR, Vaney DI. 2010. Uniformity detector retinal ganglion cells fire complex spikes and receive only light-evoked inhibition. *PNAS* 107(12):5628–33
Sivyer B, Vaney DI. 2010. Dendritic morphology and tracer-coupling pattern of physiologically identified transient uniformity detector ganglion cells in rabbit retina. *Vis. Neurosci.* 27(5–6):159–70

Smeds L, Takeshita D, Turunen T, Tihonen J, Westö J, et al. 2019. Paradoxical rules of spike train decoding revealed at the sensitivity limit of vision. *Neuron* 104(3):576–87

Sonoda T, Lee SK, Birnbaumer L, Schmidt TM. 2018. Melanopsin phototransduction is repurposed by ipRGC subtypes to shape the function of distinct visual circuits. *Neuron* 99(4):754–67.e4

Sonoda T, Li JY, Hayes NW, Chan JC, Okabe Y, et al. 2020. A noncanonical inhibitory circuit dampens behavioral sensitivity to light. *Science* 368(6490):527–31

Soto F, Hsiang J-C, Rajagopal R, Piggott K, Harocopos GJ, et al. 2020. Efficient coding by midget and parasol ganglion cells in the human retina. *Neuron* 107(4):656–66.e5

Soto F, Tien N-W, Goel A, Zhao L, Ruzycki PA, Kerschensteiner D. 2019. AMIGO2 scales dendrite arbors in the retina. *Cell Rep*. 29(6):1568–78.e4

Stabio ME, Sabbah S, Quattrochi LE, Ilardi MC, Fogerson PM, et al. 2017. The M5 cell: a color-opponent intrinsically photosensitive retinal ganglion cell. *Neuron* 97(1):150–63.e4

Stone LS, Watson AB, Mulligan JB. 1990. Effect of contrast on the perceived direction of a moving plaid. *Vis. Res.* 30(7):1049–67

Sun H, Frost BJ. 1998. Computation of different optical variables of looming objects in pigeon nucleus rotundus neurons. *Nat. Neurosci.* 1(4):296–303

Sun LO, Brady CM, Cahill H, Al-Khindi T, Sakuta H, et al. 2015. Functional assembly of accessory optic system circuitry critical for compensatory eye movements. *Neuron* 86(4):971–84

Sun W, Li N, He S. 2002. Large-scale morphological survey of mouse retinal ganglion cells. *J. Comp. Neurol.* 451(2):115–26

Suresh V, Çiftçioğlu UM, Wang X, Lala BM, Ding KR, et al. 2016. Synaptic contributions to receptive field structure and response properties in the rodent lateral geniculate nucleus of the thalamus. *J. Neurosci.* 36(43):10949–63

Szatko KP, Korympidou MM, Ran Y, Berens P, Dalkara D, et al. 2020. Neural circuits in the mouse retina support color vision in the upper visual field. *Nat. Commun.* 11:3481

Tailby C, Solomon SG, Dhruv NT, Majaj NJ, Sokol SH, Lennie P. 2007. A new code for contrast in the primate visual pathway. *J. Neurosci.* 27(14):3904–9

Tarpey P, Thomas S, Sarvananthan N, Mallya U, Lisgo S, et al. 2006. Mutations in FRMD7, a newly identified member of the FERM family, cause X-linked idiopathic congenital nystagmus. *Nat. Genet.* 38(11):1242–44

Tien N-W, Kim T, Kerschensteiner D. 2016. Target-specific glycinergic transmission from VGluT3-expressing amacrine cells shapes suppressive contrast responses in the retina. *Cell Rep*. 15(7):1369–75

Tien N-W, Pearson JT, Heller CR, Demas J, Kerschensteiner D. 2015. Genetically identified suppressed-by-contrast retinal ganglion cells reliably signal self-generated visual stimuli. *J. Neurosci.* 35(30):10815–20

Tien N-W, Soto F, Kerschensteiner D. 2017. Homeostatic plasticity shapes cell-type-specific wiring in the retina. *Neuron* 94(3):656–65.e4

Tran NM, Shekhar K, Whitney IE, Jacobi A, Benhar I, et al. 2019. Single-cell profiles of retinal ganglion cells differing in resilience to injury reveal neuroprotective genes. *Neuron* 104(6):1039–55.e12

Trenholm S, McLaughlin AJ, Schwab DJ, Turner MH, Smith RG, et al. 2014. Nonlinear dendritic integration of electrical and chemical synaptic inputs drives fine-scale correlations. *Nat. Neurosci.* 17(12):1759–66

Trenholm S, Schwab DJ, Balasubramanian V, Awatramani GB. 2013. Lag normalization in an electrically coupled neural network. *Nat. Neurosci.* 16(2):154–56

Turner MH, Sanchez Giraldo LG, Schwartz O, Rieke F. 2019. Stimulus- and goal-oriented frameworks for understanding natural vision. *Nat. Neurosci.* 22(1):15–24

Vale R, Campagner D, Iordanidou P, Arocas OP, Tan YL, et al. 2020. A cortico-collicular circuit for accurate orientation to shelter during escape. bioRxiv 2020.05.26.117598. **https://doi.org/10.1101/2020.05.26.117598**

Vale R, Evans DA, Branco T. 2017. Rapid spatial learning controls instinctive defensive behavior in mice. *Curr. Biol.* 27(9):1342–49

Van Gelder RN, Buhr ED. 2016. Ocular photoreception for circadian rhythm entrainment in mammals. *Annu. Rev. Vis. Sci.* 2:153–69

van Wyk M, Rowland Taylor W, Vaney DI. 2006. Local edge detectors: a substrate for fine spatial vision at low temporal frequencies in rabbit retina. *J. Neurosci.* 26(51):13250–63

Vitek DJ, Schall JD, Leventhal AG. 1985. Morphology, central projections, and dendritic field orientation of retinal ganglion cells in the ferret. *J. Comp. Neurol.* 241(1):1–11
Vlasits AL, Bos R, Morrie RD, Fortuny C, Flannery JG, et al. 2014. Visual stimulation switches the polarity of excitatory input to starburst amacrine cells. *Neuron* 83(5):1172–84
Vlasits AL, Morrie RD, Tran-Van-Minh A, Bleckert A, Gainer CF, et al. 2016. A role for synaptic input distribution in a dendritic computation of motion direction in the retina. *Neuron* 89(6):1317–30
Wang L, Sarnaik R, Rangarajan K, Liu X, Cang J. 2010. Visual receptive field properties of neurons in the superficial superior colliculus of the mouse. *J. Neurosci.* 30(49):16573–84
Wang Q, Burkhalter A. 2013. Stream-related preferences of inputs to the superior colliculus from areas of dorsal and ventral streams of mouse visual cortex. *J. Neurosci.* 33(4):1696–705
Wang YV, Weick M, Demb JB. 2011. Spectral and temporal sensitivity of cone-mediated responses in mouse retinal ganglion cells. *J. Neurosci.* 31(21):7670–81
Wässle H. 2004. Parallel processing in the mammalian retina. *Nat. Rev. Neurosci.* 5(10):747–57
Wee R, Castrucci AM, Provencio I, Gan L, Van Gelder RN. 2002. Loss of photic entrainment and altered free-running circadian rhythms in math5−/− mice. *J. Neurosci.* 22(23):10427–33
Wei P, Liu N, Zhang Z, Liu X, Tang Y, et al. 2015. Processing of visually evoked innate fear by a non-canonical thalamic pathway. *Nat. Commun.* 6:6756
Wei W. 2018. Neural mechanisms of motion processing in the mammalian retina. *Annu. Rev. Vis. Sci.* 4:165–92
Wei W, Hamby AM, Zhou K, Feller MB. 2011. Development of asymmetric inhibition underlying direction selectivity in the retina. *Nature* 469(7330):402–6
Weng S, Sun W, He S. 2005. Identification of ON–OFF direction-selective ganglion cells in the mouse retina. *J. Physiol.* 562(3):915–23
Yan W, Laboulaye MA, Tran NM, Whitney IE, Benhar I, Sanes JR. 2020. Mouse retinal cell atlas: molecular identification of over sixty amacrine cell types. *J. Neurosci.* 40(27):5177–95
Yao X, Cafaro J, McLaughlin AJ, Postma FR, Paul DL, et al. 2018. Gap junctions contribute to differential light adaptation across direction-selective retinal ganglion cells. *Neuron* 100(1):216–28.e6
Yilmaz M, Meister M. 2013. Rapid innate defensive responses of mice to looming visual stimuli. *Curr. Biol.* 23(20):2011–15
Yonehara K, Balint K, Noda M, Nagel G, Bamberg E, Roska B. 2011. Spatially asymmetric reorganization of inhibition establishes a motion-sensitive circuit. *Nature* 469(7330):407–10
Yonehara K, Farrow K, Ghanem A, Hillier D, Balint K, et al. 2013. The first stage of cardinal direction selectivity is localized to the dendrites of retinal ganglion cells. *Neuron* 79(6):1078–85
Yonehara K, Fiscella M, Drinnenberg A, Esposti F, Trenholm S, et al. 2016. Congenital nystagmus gene FRMD7 is necessary for establishing a neuronal circuit asymmetry for direction selectivity. *Neuron* 89(1):177–93
Yonehara K, Ishikane H, Sakuta H, Shintani T, Nakamura-Yonehara K, et al. 2009. Identification of retinal ganglion cells and their projections involved in central transmission of information about upward and downward image motion. *PLOS ONE* 4(1):e4320
Yonehara K, Shintani T, Suzuki R, Sakuta H, Takeuchi Y, et al. 2008. Expression of SPIG1 reveals development of a retinal ganglion cell subtype projecting to the medial terminal nucleus in the mouse. *PLOS ONE* 3(2):e1533
Yoshida K, Watanabe D, Ishikane H, Tachibana M, Pastan I, Nakanishi S. 2001. A key role of starburst amacrine cells in originating retinal directional selectivity and optokinetic eye movement. *Neuron* 30(3):771–80
Zaghloul KA, Boahen K, Demb JB. 2003. Different circuits for ON and OFF retinal ganglion cells cause different contrast sensitivities. *J. Neurosci.* 23(7):2645–54
Zaidi FH, Hull JT, Peirson SN, Wulff K, Aeschbach D, et al. 2007. Short-wavelength light sensitivity of circadian, pupillary, and visual awareness in humans lacking an outer retina. *Curr. Biol.* 17(24):2122–28
Zeater N, Cheong SK, Solomon SG, Dreher B, Martin PR. 2015. Binocular visual responses in the primate lateral geniculate nucleus. *Curr. Biol.* 25(24):3190–95
Zhang Y, Kim I-J, Sanes JR, Meister M. 2012. The most numerous ganglion cell type of the mouse retina is a selective feature detector. *PNAS* 109(36):E2391–98
Zhao X, Chen H, Liu X, Cang J. 2013. Orientation-selective responses in the mouse lateral geniculate nucleus. *J. Neurosci.* 33(31):12751–63

Zhao X, Liu M, Cang J. 2014a. Visual cortex modulates the magnitude but not the selectivity of looming-evoked responses in the superior colliculus of awake mice. *Neuron* 84(1):202–13

Zhao X, Stafford BK, Godin AL, King WM, Wong KY. 2014b. Photoresponse diversity among the five types of intrinsically photosensitive retinal ganglion cells. *J. Physiol.* 592(7):1619–36

Zhou Z, Liu X, Chen S, Zhang Z, Liu Y, et al. 2019. A VTA GABAergic neural circuit mediates visually evoked innate defensive responses. *Neuron* 103(3):473–88.e6

Zhu Y, Xu J, Hauswirth WW, DeVries SH. 2014. Genetically targeted binary labeling of retinal neurons. *J. Neurosci.* 34(23):7845–61

Zingg B, Chou X-L, Zhang Z-G, Mesik L, Liang F, et al. 2017. AAV-mediated anterograde transsynaptic tagging: mapping corticocollicular input-defined neural pathways for defense behaviors. *Neuron* 93(1):33–47